~~High-frequency O_2-CO_2 records reveal intensity of river metabolism and lateral exchange in the Danube Delta~~A boost on the final stretch: intense river metabolism and wetland discharge increase aquatic CO_2 dynamics in the Danube Delta

Marie-Sophie Maier[1,2,#], Bernhard Wehrli[1,2,#], Cristian R. Teodoru[3,#]

[1] Department of Surface Waters, Research and Management, Eawag, 6047 Kastanienbaum, Switzerland
[2] ~~Deparatment~~Department of Environmental Systems Science, ETH Zurich, 8092 Zurich, Switzerland
[3] National Research - Development Institute for Marine Geology and Geoecology (GeoEcoMar), Dimitrie Onciu Street 23-25, 024053 Bucharest, Romania
# The authors contributed equally to this work

Correspondence to: bernhard.wehrli@env.ethz.ch

Short summary ~~(490chars)~~

Monitoring stations in the Danube Delta revealed two orders of magnitude difference in the intensity of oxygen and carbon dioxide cycles. Biological processes were driving more intense day-night cycles ~~more intense~~ in delta channels compared to river reaches and were mainly ~~driven~~ controlled by changes in temperature and cloud cover. ~~Spring floods transferred wetland water to downstream river reaches. The statistical analysis of sensor data provided insights into timing, intensity and type of processes in this complex coastal system.~~Wetland discharge added dissolved CO_2 from anaerobic processes and caused higher emission rates in delta channels and downstream river reaches.

Abstract

~~Due to their intense terrestrial-aquatic linkages and intense ecosystem metabolism, many~~Many river deltas are aquatic hot spots for carbon dioxide (CO_2) emissions to the atmosphere. ~~A~~ Their patchwork of wetlands, lakes, channels, and river reaches often complicates the analysis of CO_2 sources such as ecosystem respiration or lateral water transfer. Sensing techniques offer the opportunity of measuring the ~~paired~~ CO_2, O_2 and DIC concentrations at high temporal resolution for periods from days to months. Such time-series allow ~~quantifying~~ quantification of diurnal and seasonal cycles of river metabolism and lateral exchange. This study addresses the following general hypotheses: (1) Ecosystem metabolism intensifies when river water enters the slower flow paths through channels and lakes of a delta. (2) Wetland discharge from a delta significantly alters the oxygen and carbon dynamics in a river. ~~This~~ (3) In such a case, average aquatic CO_2 emissions increase on the final stretch before a river reaches the sea. ~~study documents~~We tested these hypotheses based on ~~paired O_2-CO_2~~ measurements of the oxygen and carbon dynamics at 15-minute time resolution obtained from ~~deployment of~~ sensor packages. They were deployed for two years in the three main river reaches ~~and channels~~ of the Danube Delta in Romania ~~during a total observation period of three years~~and for an additional year in three channels within the delta. ~~We show how to combine~~By combining ~~results from~~ covariance analysis ~~with~~ and ~~insights from averaged~~monthly averaging of 24-hour ~~diurnal~~ cycles~~. The time series reveal~~ we found a factor 100 difference in the ~~two orders of magnitude variability~~ amplitude ~~in~~ of daily O_2 and CO_2 fluctuations ~~along the main Danube reaches with typical maxima in the early morning and minima in the afternoon~~across different stations and seasons. Channels with slow flow paths within the delta exhibited 4-8 times larger median amplitudes in daily metabolic cycles compared to the upstream river station. Correspondingly, metabolic intensity was on average 3-4 times more sensitive to changes in water temperature and cloud cover within the delta compared to the main river. Discharge of O_2-depleted and CO_2-rich wetland water into the downstream river sections was most pronounced during spring floods ~~The amplitude of monthly averaged daily cycles was 2-2.5 times larger in delta channels compared to the river reaches and the parameter for metabolic intensity reacted on average four times more sensitive to changes in water temperature and cloud cover within the delta compared to the main river. Inflow of O_2-depleted and CO_2-rich wetland water to the downstream river stations was most intense during spring floods~~ with ~~estimated~~ apparent mixing rations of up to ~~5-20~~13-25% depending on the station. ~~Stoichiometry of O_2-CO_2 changes pointed to strong contributions of methane oxidation and/or nitrification in 40% of the analysed summer data, which was also evident from the frequently observed oxygen deficiency. During June July, a monitored lake system and an adjacent channel showed clear evidence for calcite precipitation and a switch to photosynthetic uptake of HCO_3^-. The study illustrates the benefits of a combining covariance analysis with 24 hours averaging for identifying the timing, intensity and type of processes in river metabolism and lateral exchange.~~ In a delta channel draining wetland waters, average CO_2 supersaturation was almost an order of magnitude higher than in the Danube inflow. ~~The~~ combined effects of intense metabolism within the delta and wetland discharge doubled the CO_2 emissions near the river mouth compared to an upstream Danube station. At the landscape level, however, carbon drawdown is likely five times larger than aquatic CO_2 emissions. Based on a high-resolution timeseries spanning three years, this study demonstrates how connected wetlands enhance aquatic metabolism and associated CO_2 dynamics in a large, lowland river.

1. Introduction

Over the last decades, the paradigm of river systems as active reactors (Cole et al., 2007) replaced a pipe model for carbon and nutrient transfer from land to ocean (Degens et al., 1984). Global estimates of CO_2 emissions from rivers and streams are 1.8 ± 0.25 petagrams of carbon per year (Raymond et al., 2013). ~~Adding~~ Including wetlands and inundated areas to river corridors (Abril and Borges, 2019) has further improved the analysis of carbon (Zuijdgeest et al., 2016) and oxygen dynamics in rivers (Zurbrügg et al., 2012). Reviews of river metabolism (Hotchkiss et al., 2015) covering the land-ocean aquatic continuum from the headwaters to the coastal zone ~~collected~~ have compiled an extensive database of carbon fluxes and transformations for ~~large~~ river systems but available data remain more limited for large rivers and for ~~in~~ the heterogeneous environments of the coastal and deltaic zones. Estuaries and their coastal vegetation were recently recognized as an effective global carbon sink (Rosentreter et al., 2023) ~~and the risks from coastal change by erosion, subsidence, sea level change and hydraulic modification (Renaud et al., 2013) call for more detailed analyses of actual carbon dynamics in river deltas.~~ but lateral carbon transfer from wetlands plays a key role in CO_2 emissions of large river systems (Hastie et al., 2019). Our study aims to clarify the role of a large river delta in modifying the intensity of the regional river metabolism and the associated CO_2 emissions.

Because river deltas often enclose large wetlands, the final stretch of a large river before entering the sea may exhibit a markedly different carbon dynamics compared to the upstream part. Three hypotheses guided this study on the delta of the Danube River in Romania: (1) Ecosystem metabolism intensifies when river water enters the slower flow paths through channels and lakes of a delta. (2) Wetland discharge from a delta significantly alters the oxygen and carbon dynamics in a river. (3) In such a case, average aquatic CO_2 emissions increase on the final stretch before a river reaches the sea.

~~Compared to smaller streams,~~Testing these hypotheses requires ~~the~~ monitoring and analysis of ecosystem metabolism in large river sections and small wetland channels, each with specific characteristics ~~in large river sections faces both advantages~~ and challenges (Bernhardt et al., 2017): wide river sections with ~~large~~ extensive open water areas are typically not shaded by riparian vegetation which reduces the seasonal effects of ~~leave~~ leaf cover. Furthermore, hydrological changes occur more ~~slowly~~ gradually and with ~~smaller~~ lower amplitude compared to headwater streams where disturbance regimes may induce abrupt ecosystem change such as the abrasion of productive biofilms (Sabater et al., 2016). On the other hand, ~~dynamic flooding of adjacent wetlands and~~ lateral groundwater exchange in large river corridors and dynamic flooding of adjacent wetlands may play an ~~more~~ important role for CO_2 emissions ~~than the daily oscillations of in-stream metabolism~~(Borges et al., 2019; Marzolf et al., 2022). ~~(Borges et al., 2019), (Marzolf et al., 2022).~~ Wetlands are biogeochemical hotspots with high rates of daily gross primary production (Rabaey et al., 2024). Therefore, estimates of CO_2 concentrations and their potential drivers in lowland rivers (Reiman and Xu, 2019) and river deltas (Huertas et al., 2017) ~~could~~ can be improved by high-frequency measurements that allow resolving diel and seasonal cycles of photosynthesis, respiration, and transfer across system boundaries (Battin et al., 2023).

Progress in sensor technology (Rode et al., 2016) now facilitates the autonomous registration of water quality parameters at high frequency over time periods of months. Seasonal and multi-annual observations are feasible with appropriate maintenance and calibration. Specifically, wetland connectivity (Maier et al., 2022), the role of seasonal flood pulses (Dalmagro et al., 2018) and differences between daytime and nocturnal emissions (Gomez-Gener et al., 2021) can be monitored by in situ sensors. Covariance analysis of paired O_2 and CO_2 measurements from sensor deployments provides insights into the biological, chemical and physical forcing of aquatic ecosystem

processes over time (Vachon et al., 2020). Analysing the temporal dynamics of paired O_2-DIC measurements offers the advantage of removing buffer effects and simplifying carbon budget calculations (Shangguan et al., 2025). This combination of sensor measurements with statistical analysis has proven highly valuable in recent studies (Rocher-Ros et al., 2025) for identifying drivers of CO_2 dynamics in US rivers (Delvecchia et al., 2023) and in the lower Ganges (Haque et al., 2022), for assessing the balance between river metabolism and CO_2 emissions (Solano et al., 2023), for identifying the contribution of lateral inputs to the carbon budget of rivers (Marzolf et al., 2022), and for calculating the fraction of bicarbonate that supports river photosynthesis (Aho et al., 2021).

This study in the Danube Delta builds on previous analyses of discrete monthly sampling campaigns ~~over the period of~~during two years (Maier et al., 2021) which revealed median CO_2 fluxes in the main branches of the Danube of 25 mmol CO_2 m^{-2} d^{-1}, and four times higher values in the canals connecting wetlands and lakes. A subsequent on-site mapping study of dissolved gases at high spatial resolution by membrane-inlet mass spectrometry (Maier et al., 2022) revealed hot-spots in emission rates caused by wetland ~~water entering~~discharge to the canal systems, by plant mediated gas transfer via O_2 ebullition in lakes, and by excess air formation in reed stands. Here we report results from a two-year deployment of commercially available multiprobe ~~EXO2~~ sensors (YSI EXO2) recording every 15 minutes in the three main stems of the Danube in the Romanian part of the delta near the Black Sea coast which was followed by a one-year deployment in selected delta channels ~~of the delta~~. ~~The sensors measured temperature, conductivity, dissolved oxygen and pH. Dissolved CO_2 was calculated from a correlation of conductivity with alkalinity and from the recorded pH and temperature data. The different O_2-CO_2 time series characterized diverse processes in main river reaches, and in the delta with its reed stands, channels and lakes. To assess the temporal dynamics, we performed covariance analyses of daily and monthly O_2-CO_2 patterns (Vachon et al., 2020) and calculated mean 24 hour cycles of O_2-CO_2. We addressed the questions which potential physical drivers, such as temperature, irradiation, and runoff, govern the variability of dissolved CO_2 and O_2 at daily and monthly time intervals and which biogeochemical processes such as photosynthesis, respiration, methane oxidation or calcite precipitation were shaping the O_2-CO_2 cycles. On a methodological level, we analysed the merits and limitations of covariance analysis and averaged 24 hour cycles for gaining process level insights from paired O_2-CO_2 observations.~~Time series of dissolved O_2, CO_2 and DIC obtained from these campaigns allowed us to address the following specific research questions: (1) How does the intensity of river metabolism differ between the open waters of the delta compared to the upstream Danube River? (2) How significant is the contribution of lateral inflows from lake systems and reedbeds to the O_2 and CO_2 dynamics of the main river reaches crossing the delta? (3) What are the overall effects of river metabolism and wetland discharge on aquatic CO_2 emission rates in the Danube Delta–? By addressing these questions our study demonstrates how high-frequency observations can identify the controls of carbon processing and aquatic CO_2 emissions in large, heterogeneous river deltas. The results fill a gap in our understanding how wetland–river interactions may define carbon dynamics on the final stretch of the land–ocean aquatic continuum.

2. Materials and Methods

2.1 Study site and monitoring stations

The Danube River is the second largest river in Europe and its international catchment of 817,~~'~~000 km^2 covers parts of 19 European countries. ~~(River, 2018).~~ Originating in the Black Forest Mountains in Germany, the Danube

flows southeast for over 2,~~'~~857 km before discharging into the Black Sea. The ~~annual average flow rate~~long-term mean discharge is 6,360 m^3 s^{-1} and ranged from ~~2'930~~ 2,930 m^3 s^{-1} to ~~11'300~~ 11,300 m^3 s^{-1} in the period 1921-2015 at the Ukrainian station of Reni (Romanova et al., 2019). Receiving meltwater from the Alps and the Carpathian Mountains, the hydrology of the Danube River ~~has~~ shows a pronounced seasonality. In general, peak discharge lasts from April to June and low flow conditions prevail between September and November. Driven by rainfall in the lower catchment, a~~A~~ secondary ~~maximum in~~ discharge maximum usually occurs from December through January. ~~due to rainfall in the lower catchment (Fig. 1a).~~ During our study, s~~S~~easonal air temperature changes varied from around ~~zero~~ 0 °C in winter to 20-25°C in summer. The probability of cloud cover was higher in winter than in summer (Fig. 1a).~~.~~

Close to the mouth, the river splits into three arms that form the Danube Delta: Chilia in the north constitutes the border with Ukraine, Sulina in the middle was modified for maritime commercial navigation while ~~Sfantu~~ Sfântu Gheorghe (St. George) limits the delta area in the south (Fig. 1b). The surface area of the Danube Delta between these river reaches is approximately 4,150 km^2, of which more than 80% ~~is part of~~lies within Romania~~n territory~~. As the youngest and the longest among the three arms, the 120 km long Chilia branch carries more than 50% of the Danube water, the 64 km long Sulina channel about 27% and the 70 km long river reach of St. George contributes about 20% to the total water discharge ~~into the Black Sea~~. Travel-time analysis based on our sensor data resulted in average flow velocities in the range of 0.7 ~~and~~ 1.0 m s^{-1}.

An intricate network of approximately 470 lakes, swamps, shallow water pools and about 3,500 km of channels connects the delta's wetlands with the ~~river~~Danube River (Gomez-Baggethun et al., 2019). Although considered the most pristine delta in Europe, a series of hydrotechnical works in the Danube Delta, mostly for agriculture and fishery, ~~lead~~ led to doubling the length of the internal canals after 1980 (Gatescu et al., 1983). This, in turn, gradually increased the water flow through the delta from 260 m^3 s^{-1} between 1951 and 1960 to 620 m^3 s^{-1} in the period 1981-1990 (Bondar, 1994). Today, approximately 10% of the total Danube discharge is ~~considered~~ estimated to enter the delta, of which about 20% (~120 m^3 s^{-1}) may be lost via evapotranspiration in the wetlands ~~and its reed stands~~. Reed (*Phargmites australis*) is the dominant species in the Delta covering ~ 1,600 km^2 or almost 40% of the study area (Oosterberg et al., 2000). Large stretches of the channels are bordered by riparian forests composed mainly of black alder (*Alnus glutinosa*) and silkvine (*Periploca graeca*) (Oprea et al., 2024). Most of the lakes are eutrophic and classified into three types: (1) lakes at short distance to the river with high flushing rates and dense submerged vegetation, (2) large, relatively deep lakes like Puiu and Rosu with longer residence time and high *Potamogeton*-cover that collapses during winter, and (3) small, isolated lakes receiving "black-water" inflows from floating reedbeds and dominated by~~:~~ *Ceratophyllum demersum* and *Nitellopsis obtusa* (Coops et al., 2008). A high diversity of submerged and floating macrophytes is present in the canals and old meanders (Oosterberg et al., 2000).

In the first phase of this study, we deployed four sensor packages (EXO2 Multiparameter Water Quality Sondes, YSI) ~~in~~ along the main branches of the Danube ~~River~~ at the stations labelled Tulcea, Chilia, Sulina, and St. George (Fig. ~~1a~~1b). Tulcea served as the upstream reference station for water entering the delta. The Chilia branch receives additional input from a Ukrainian catchment with shallow lakes to the north, the Sulina channel serves as the main shipping route with lateral inputs from adjacent wetlands, and the St. George branch collects inflow mainly from wetlands on its left side. The monitoring stations recorded data every 15 minutes between November 2015 and February 2018. For consistency, all timestamps were recorded in Easter European Time (EET) without a switch to summertime (EEST). For further details on time intervals and locations see ~~(~~Fig. A1 and~~,~~ Table A1~~)~~. One

multiprobe was damaged by ~~the~~ floating ice in December 2016 which ~~shortened~~ limited the time series at Chilia station to one year. In the second phase from February 2018 to December 2018, the remaining three EXO2 probes were installed in channels within the delta at ~~stations Balanova, Busurca and~~ Puiu-Rosu, Balanova and Busurca. Puiu-Rosu is influenced by outflow of a large and relatively deep lake complex, Balanova receives mixed input from lakes wetlands while Busurca is mainly connected to reedbeds with negligible lake influence. Note that Balanova ~~is~~ refers to a local name ~~for a site on~~along the Central Channel that connects the Sulina and St. George branches (Fig. 1b).

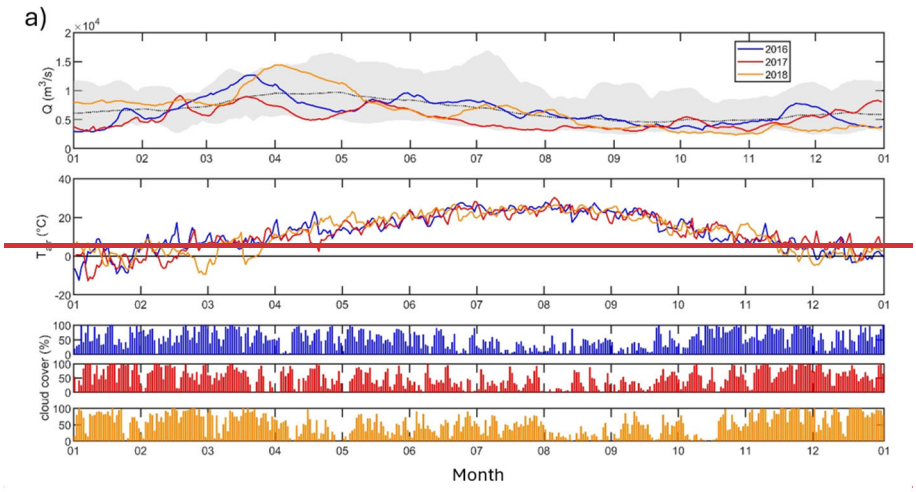
a)
Q (m³/s)
2016
2017
2018
T_air (°C)
cloud cover (%)
Month

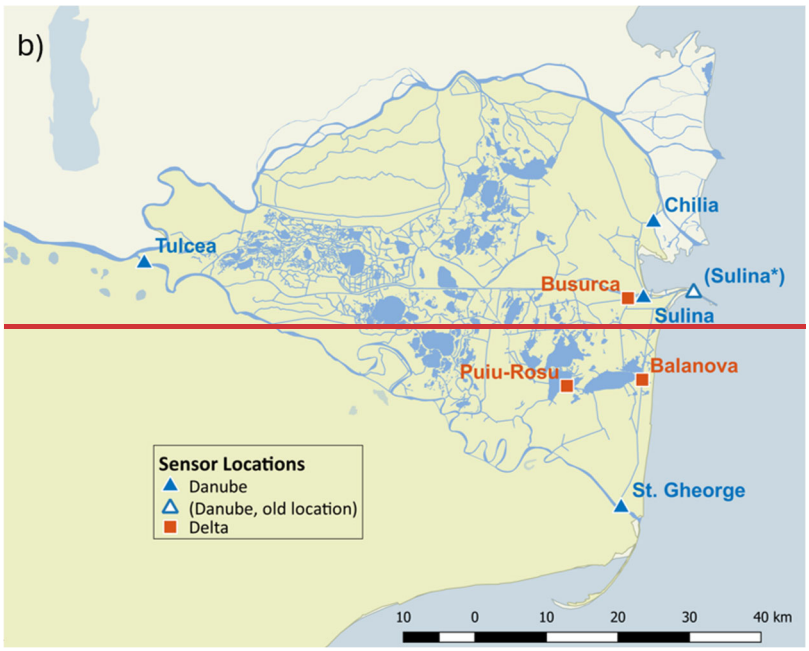
b)
Tulcea
Chilia
Busurca
(Sulina*)
Sulina
Puiu-Rosu
Balanova
St. Gheorge
Sensor Locations
Danube
(Danube, old location)
Delta
10 0 10 20 30 40 km

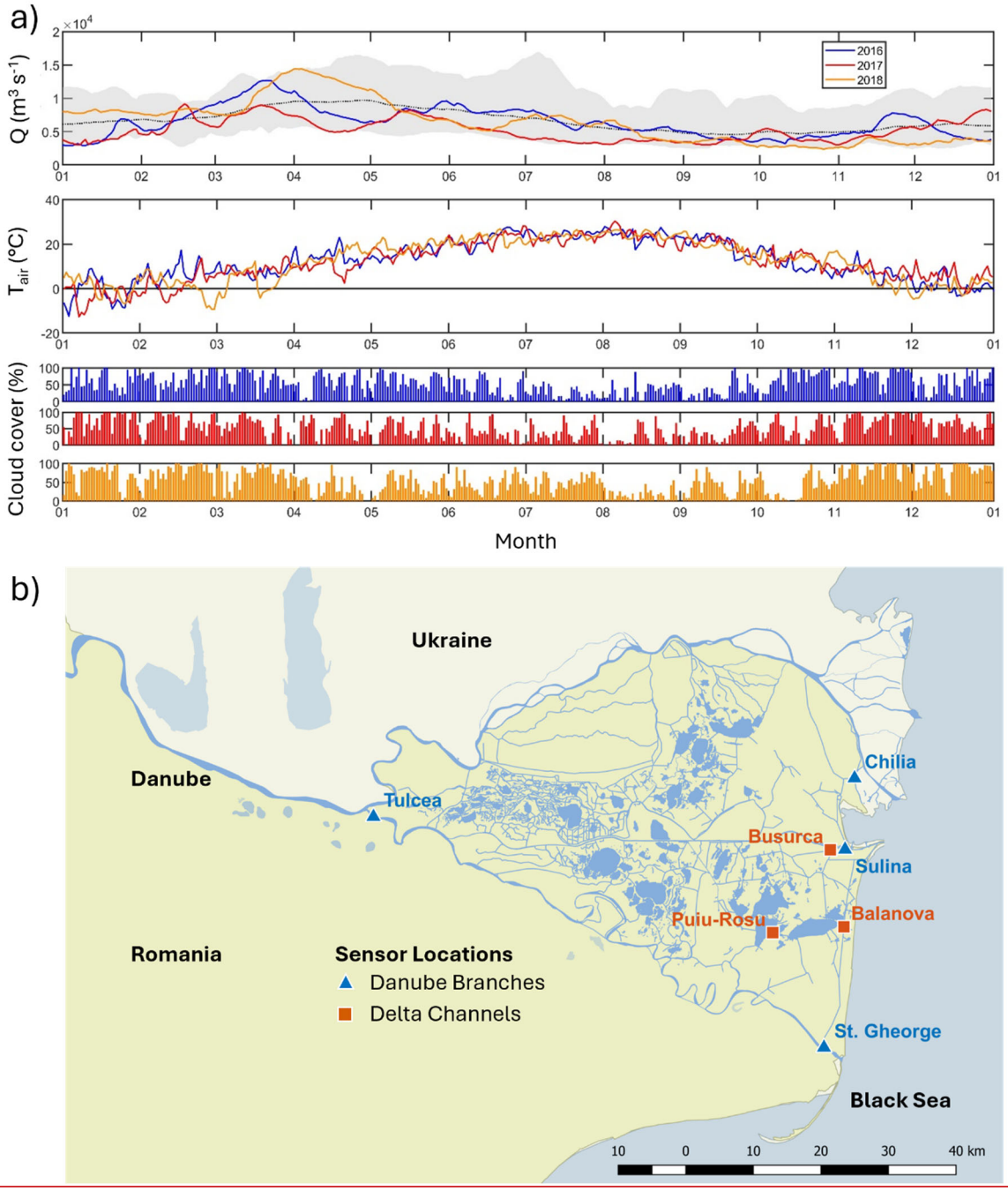

205 ***Figure 1a)*** *–Three years of environmental records for the Danube Delta 2016-2018. Top: ~~average~~ mean daily discharge of the Danube at Reni, Ukraine, upstream of the Delta (available at https://www.danubehis.org/stations - last access 27. Oct. 2025). Gray area ~~shows~~ indicates the range of daily discharge for the period 1998-2017. Middle: average daily air temperature; bottom: average daily cloud cover at Tulcea Airport (available at https://rp5.lv/Weather_in_Tulcea_(airport) – last access 27. Oct. 2025).* ***b)*** *Monitoring locations for EXO2 probes*

210 *in main branches and within the Danube Delta~~, the old location refers to Sulina station in 2016, which was relocated in 2017~~. Map: © OpenStreetMap contributors 2024. Distributed under the Open Data Commons Open Database License (ODbL) v1.0.*

2.2 Measured and derived parameters

The EXO2 multiprobe sensors recorded water temperature, pH, specific conductivity, and dissolved oxygen every 15 minutes. ~~The output~~Data of ~~additional~~ sensors for turbidity and fluorescent dissolved organic matter ~~(fDOM) were~~ was not analyzed for this study. Before each measurement, the ~~individual~~ sensor caps were automatically cleaned ~~automatically~~ by a wiper. The EXO ~~sensors~~ probes were moored at approximately 1 m below the water surface. Data gaps ~~in the time series~~ occurred sporadically due to unexplained energy drain from batteries and when probes were removed to prevent damage by floating ice sheets during cold spells in winter. Once a month, the probes were removed from the water ~~and cleaned~~for cleaning and pH and O_2 sensors were calibrated using standard buffer solution and air-saturated water, respectively. Post-deployment, the data was drift-corrected using the calibration data. Crosschecks with discrete in situ measurements using the YSI Optical Dissolved Oxygen and Professional Plus Multiparameter ~~sensors~~ instruments (Maier et al., 2021) showed good agreement. We used a low conductivity threshold (< 200 µS cm^{-1}) to detect and delete invalid data points ~~measured~~ recorded at times when the sensor was out of the water for servicing.

We derived the alkalinity time series from specific conductivity data using the linear correlation ~~(Maier et al., 2021)~~ between laboratory analysis of alkalinity and specific conductivity (SpCond) measurement as: alkalinity [mmol L^{-1}] = 0.0057~~*~~×SpCond [µS cm^{-1}] + 0.60 (R^2 = 0.70, Fig. B1). The same approach has been applied to derive multidecadal trends for CO_2 evasion in the Loire River (Nguyen et al., 2025) and to estimate global riverine CO_2 emission rates (Raymond et al., 2013). To calculate CO_2 from pH and alkalinity, we used the CO2SYS MATLAB code version 1.1 with Matlab R2017a and 2022b (Van Heuven et al., 2011). These calculations were based on ~~the~~ dissociation constants ~~from (Cai and Wang, 1998)~~ for a temperature range of 2°C to 35°C ~~and a salinity from 0 to 49~~(Cai and Wang, 1998)~~;~~. To obtain an upper and lower estimate for the derived CO_2 time-series, we propagated the uncertainty ~~related to~~of the alkalinity-conductivity regression estimates and obtained an error of ± 13%. The calculated CO_2 values correlated well with discrete headspace measurements taken at the same time and location (R^2 = 0.82, Fig. B1). Finally, we used solubilities (Weiss, 1974) and the temperature recordings from the EXO2 probes to calculate the deviation from atmospheric equilibrium in µmol L^{-1} of the O_2-CO_2 pairs. We defined the frequent excess of CO_2 and the typical deficit of O_2 with regards to atmospheric equilibrium as $exCO_2$ and exO_2 [µM] with a positive or negative sign, respectively~~, and we determined the dissolved concentrations in the µM range~~. For the correlation of ~~this~~ daily O_2-CO_2 ~~time series with~~covariance data with potential physical drivers, we used averaged daily water temperature from the EXO2 sensors and cloud cover from a meteorological station in Tulcea ~~meteorological and hydrological conditions we used hourly data from a meteorological station in Tulcea covering the years 2015–2019~~ (Fig. 1a). The time-shift of one hour during daylight saving time was removed to synchronize the meteorological data with the continuous recording of EXO probes. ~~Daily averages of air temperature and cloud cover as a proxy for reduced irradiation were used as potential physical drivers for river metabolism and water levels at Tulcea were tested as potential drivers for lateral exchange between wetland and river system.~~

Some data-~~cleanup~~ filtering was necessary for the time series of Chilia (2016) ~~and Sulina (2017)~~ which ~~were~~ was sporadically influenced by water from an adjacent wetland and for Sulina (2017) which recorded disturbances from the Black Sea, respectively~~, which lead to steep increases in specific conductivity (spike events).~~. We flagged these ~~points as~~ spikes in conductivity by comparing the time series with upstream Tulcea station and removed data

if ~~the data~~they deviated more than 40 µS cm^{-1} from the baseline. This approach missed the beginning and the end of the spike events. To refine the cleanup, we took 5 hours before and after an identified spike event and eliminated periods with changes in specific conductivity larger than 2 µS cm^{-1} and completed the task with few manual adjustments.

2.3 Statistical analysis

Vachon et al. (2020) proposed a set of parameters obtained from covariance analysis of paired exO_2-$exCO_2$ measurements to gain insights into aquatic ecosystem metabolism. Because buffer effects may distort the exO_2-$exCO_2$ data clouds at low CO_2 concentrations(Shangguan et al., 2025; Diamond and Bertuzzo, 2025; Diamond et al., 2025) (Diamond et al., 2025; Nguyen et al., 2025), we included the DIC timeseries and paired exO_2-DIC measurements in our analysis. We ~~implemented this approach with~~developed a workflow in Mathematica 14.~~0~~ 3 to analyze the Danube Delta time series at monthly and daily timescales. Days with ~~less~~ fewer than 85 data pairs were excluded from analyses, as typically 96 pairs were recorded daily at 15 minutes intervals. Monthly analyses usually involved more than 2800 pairs and ~~datasets~~ months with less than 500 pairs were ~~excluded from further analysis~~omitted. Results of the covariance calculations included ~~The~~ the centroids which represent the mean of the exO_2 and $exCO_2$ data over the period of days or months ~~,~~and the offset of the mean from an ideal line with slope -1 for photosynthesis and respiration (Fig. 2a). Stretch and width were obtained from the Eigenvalues of the covariance matrix as the major and minor axes length of the 95% ~~error~~ confidence ellipse ~~(Fig. 2a)~~ and ~~W~~we obtained the slope s_{cov} of the stretch-line from the Eigenvectors of the covariance matrix. ~~. As an extension to the proposal of Vachon et al. (20220), we defined a negative sign for the offset if the centroid was located below the 1: 1 line (Fig. C1). We obtained the slope s_{cov} of the stretch-line from the Eigenvectors of the covariance matrix. The Eigenvector approach worked even for almost circular patterns with a stretch to width ratio < 4.0, when a reduced mean axis (RMA) regression algorithm failed to converge.~~

Parameters for the 95%-ellipses obtained from covariance analysis provide valuable insights into the intensity of photosynthesis and respiration (stretch), the ecosystem quotient (EQ = 1/slope), and the impact of ~~confounding processes such as~~ lateral inflow~~s or microbial processes~~ (centroid position, offset). ~~These confounding processes often obscure the dynamics of photosynthesis and respiration at monthly timescales.~~

To analyse monthly day-night dynamics, we calculated the average 24 hours day-night cycles for each month of sensor deployment. For instance, monthly averages for 8 am in June were obtained by taking the mean of all June measurements at 8:00, 8:15, 8:30 and 8:45. This approach resulted in average timing and amplitudes ~~of daily O_2-CO_2 cycles~~of the exO_2, $exCO_2$ and DIC cycles. ~~These~~ The time-of-day averages reduced the ~~weight~~ influence of outliers and resulted in slopes s_{24} that may reflect EQs more closely than the tilt of the monthly covariance ellipse (s_{cov}) ~~which is co-defined by lateral inflows~~ (Fig. 2b). ~~Comparing the 105 available monthly records showed that s_{24} slopes from 24 h monthly averages were in general steeper than s_{cov}. The median ratio of s_{24} : s_{cov} was 1.56 (Fig. C2).~~ The following analysis, however, focuses on amplitudes and stretch as indicators of metabolic intensity and on the offset and centroid positions as indicators of wetland discharge.

For a more detailed analysis, boxplots of the amplitudes of exO_2, $exCO_2$, DIC and stretch parameters were based on all available monthly data at the seven stations (Table A1). The boxes show the median and quartiles (25 and 75%), whiskers indicate the range of values (excluding outliers). The statistical difference of these parameters for metabolic intensity between river and delta stations was evaluated by Kruskal-Wallis tests. To assess the influence of temperature and daylight on the aquatic ecosystem metabolism, stretch parameters from daily covariance

analyses were correlated by linear regression and covariance analysis with average daily cloud cover data from Tulcea Airport and water temperature measured in-situ by the EXO2 probes.

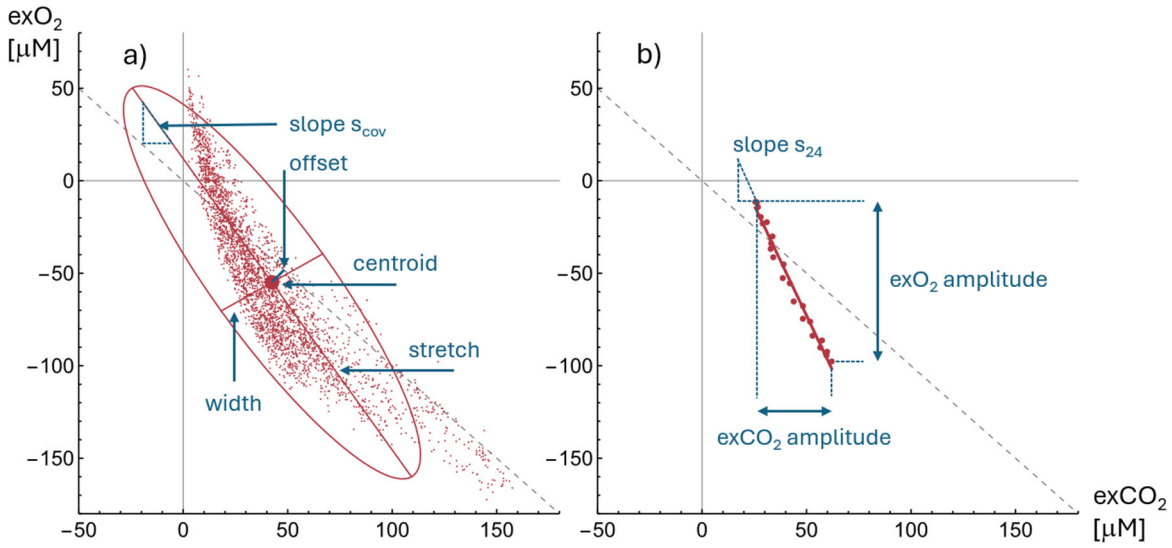

Figure 2 a) *Example of covariance analysis of ~~$exCO_2$~~ exO_2 $exCO_2$ data from July 2018 at Balanova station. Small dots are individual data points acquired every 15 minutes~~, the large dot marks the centroid, i.e. the mean $exCO_2$ and exO_2 concentration of the month~~. The ellipse encloses 95% of the datapoints and is ~~constructed~~ defined by ~~with~~ the centroid and the two main axes (125 and 29 µM) ~~calculated~~ derived from the Eigenvalues of the covariance matrix. ~~The covariance slope s_{cov} (−1.56) is calculated from the Eigenvector of the covariance matrix.~~ The offset ~~is calculated as~~corresponds to the nearest distance of the centroid from the grey dotted line with ~~−1 slope~~a slope of -1 for a theoretical photosynthesis-respiration ~~metabolism~~process. **b)** Using the same data as in a), the monthly averages over 24 hours of the day define a mean daily cycle for July at Balanova station. ~~The 24-h slope s_{24} in this example is −2.4.~~ The average daily cycle shows an $exCO_2$ amplitude of 36 µM but a wider exO_2 amplitude of 88 µM~~, with a maximum oxygen deficit at 6:30 AM and an exO_2 maximum at 4:30 PM (compare Fig. 3).~~)*

3. Results

3.1 ~~Daily fluctuations of carbon dioxide and oxygen~~Intensity of river metabolism

~~The~~ The intensity of photosynthesis and respiration, as recorded by CO_2 oversaturation with respect to atmospheric equilibrium, O_2 deficits and DIC concentrations, varied strongly in space and time during the observation period. The~~lower Danube shows consistent oversaturation with respect to CO_2 and significant oxygen deficits compared to atmospheric equilibrium.~~ inflowing Danube at Tulcea showed DIC minima of 2.6 mM in the warm season and maxima of 3.5 mM during the cold months (Fig. C1). ~~To provide an overview of the $exCO_2$ and exO_2 dynamics in the Danube and its delta, at both seasonal and daily timescales, we calculated the monthly averaged diel~~

~~fluctuations (Fig. 3, Fig. D1). Before splitting into three branches that confine the area of the delta, the Danube~~
~~River at Tulcea~~ Averaging the 24-hour cycles for O_2, CO_2 and DIC at the monthly scale provided insights into the intensity and seasonality of river metabolism (Fig. 3, Fig. C2). In~~station~~ 2017 ~~shows~~ the sensors at Tulcea recorded ~~only a~~ small and rather constant supersaturation ($exCO_2$) and undersaturation (negative exO_2) ~~over day night cycles and seasons~~in the range of ± 40 µM ~~.~~ with diel amplitudes from ~1 µM in the cold months and below 10 µM in the warm season. Within the delta, the 24-h cycles at Balanova channel showed maximum daily fluctuations of more than 100 µM for exO_2 in August. Overall, the 24-h amplitudes spanned two orders of magnitude between the extremes of 1 µM for the cold season in the upstream Tulcea station and 100 µM for warm season amplitudes within the delta.

The Balanova observations were characterized by maxima in the early morning (6-8 AM) and minima in the afternoon (4-6 PM) between April and November (Fig. 3). Compared to $exCO_2$, the oxygen cycles represented a mirror image where the strong undersaturation in the morning hours relaxed to near-equilibrium conditions in the late afternoon. Compared to CO_2 and O_2, the 24-h DIC curves showed more stochastic deviations from the sinusoidal pattern, likely reflecting the rapidly changing DIC concentration in the inflow (Figs. C1, C2).

~~Deviations from equilibrium concentrations were mostly confined to + 20 – 40 µM. Exceptions occurred in June 2016 and from May to June 2017, when O_2 was oscillating with a low average amplitude of 6-9 µM close to equilibrium, which was an indication for in-stream photosynthesis (Table 1). The downstream locations of Sulina (2016) and St. George showed strong CO_2 supersaturation with concentrations increasing from summer to autumn (Fig. D1). During the warm season, exO_2 in St. George and Chilia were marked by significant diel cycles of 20–30 µM~~

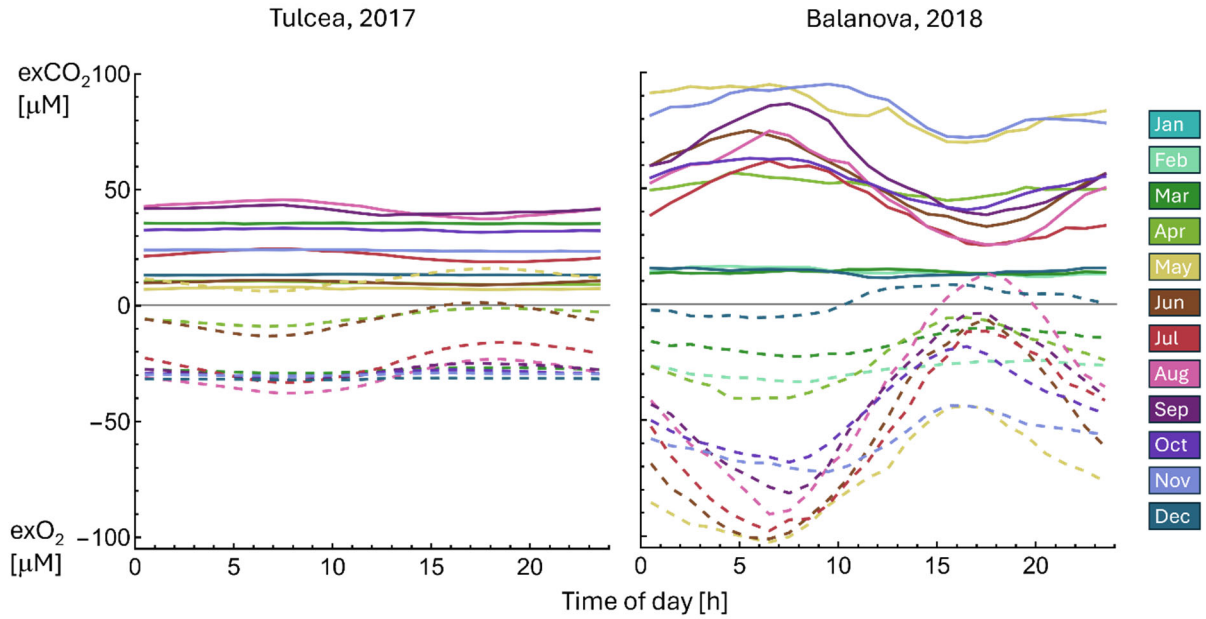

Figure 3. *Examples of 24-h monthly averages of $exCO_2$ (solid lines) and exO_2 (dashed lines) at Tulcea from March to December 2017 and at Balanova station from February to December 2018. The averaged daily cycles define characteristic amplitudes and timing of river metabolism for each month. See Fig. C2 for corresponding 24-cycles of DIC.*

~~.~~ A comparison of median 24-h amplitudes based on four indicators of metabolic intensity (amplitudes of exO_2, $exCO_2$, DIC and the stretch parameter from covariance analysis) revealed significant differences between sites

(Fig 4). The two downstream sites of St. George and Chilia showed consistently higher median amplitudes compared to Tulcea. Amplitudes of $exCO_2$ were generally lower than those of exO_2, whereas the 24-h DIC variability was typically higher. Overall, ~~These strong differences in the level and daily amplitude of~~the daily metabolic cycles intensified on ~~CO_2 and O_2 building up in~~ the final ~60 ~~to~~ to 120 km of river flow ~~from~~ between Tulcea ~~to~~ and the three ~~near shore~~near shore ~~stations indicated important inflows from the Danube Delta wetlands~~stations. ~~at these stations.~~

~~The observations within the Delta in 2018 provide information on typical concentration ranges of CO_2 and O_2 in these lateral inflows. While the concentrations in the winter months remained close to the values of Tulcea, the CO_2 curves show strong daily oscillations. For consistency, the timing is clocked by Easter European Time (EET) without a shift to summertime (EEST). Dynamics at the Balanova station was characterized by maxima in the early morning (6-8 AM) and minima in the afternoon (4-6 PM) between April and November (Fig. 3). Compared to CO_2, the oxygen curves represented a mirror image where the strong undersaturation in the morning hours relaxed to equilibrium values in the late afternoon. The amplitude of these average daily oscillations reached maxima of 49 and 104 µM for $exCO_2$ and exO_2, respectively (Table 1). By contrast, the outflow of the lake complex Puiu Rosu was closer to atmospheric equilibrium (Fig. D1) and had smaller $exCO_2$ concentrations and daily amplitudes up to 19 µM. Also, exO_2 from the lake complex showed oscillations occurring close to equilibrium but with amplitudes like Balanova (up to 108 µM). The Busurca Channel represented an extreme case because it drains significant amounts of wetland water~~Compared to the river stations, amplitude and stretch values recorded in the delta were significantly larger ($p < 0.01$ for exO_2, $exCO_2$ and stretch, $p \sim 0.01$ for DIC). ~~. As a result, the monthly average of the daily patterns showed CO_2 levels around 300 µM in February-March and reached almost 500 µM in May and July, when the O_2 concentrations approached anoxic condition~~Overall,~~s~~ the average daily fluctuations revealed increasing median values in the amplitude of exO_2 from the apex to the inner delta, with low values from 6.5 and 4.5 µM at Tulcea and Sulina, respectively, to higher amplitudes of 29 and 9.3 µM at St. George and Chilia and consistently high values within the delta (28, 50, and 29 µM in Puiu-Rosu, Busurca and Balanova). In terms of median amplitudes, metabolic activity per unit volume was thus about 4-8 times higher at stations within the delta than at the upstream station of Tulcea. A similar pattern was observed for the median DIC amplitudes with 13 and 12 µM in Tulcea and Sulina, 50 and 23 in St. George and Chilia and elevated values within the delta: 23, 32 and 40 µM at Puiu-Rosu, Balanova and Busurca, respectively. Using DIC as an indicator, metabolic activity within the delta was 2-3 times higher than at the upstream Danube station. The results demonstrate how river metabolism intensified in the slow-flowing waters of the delta.

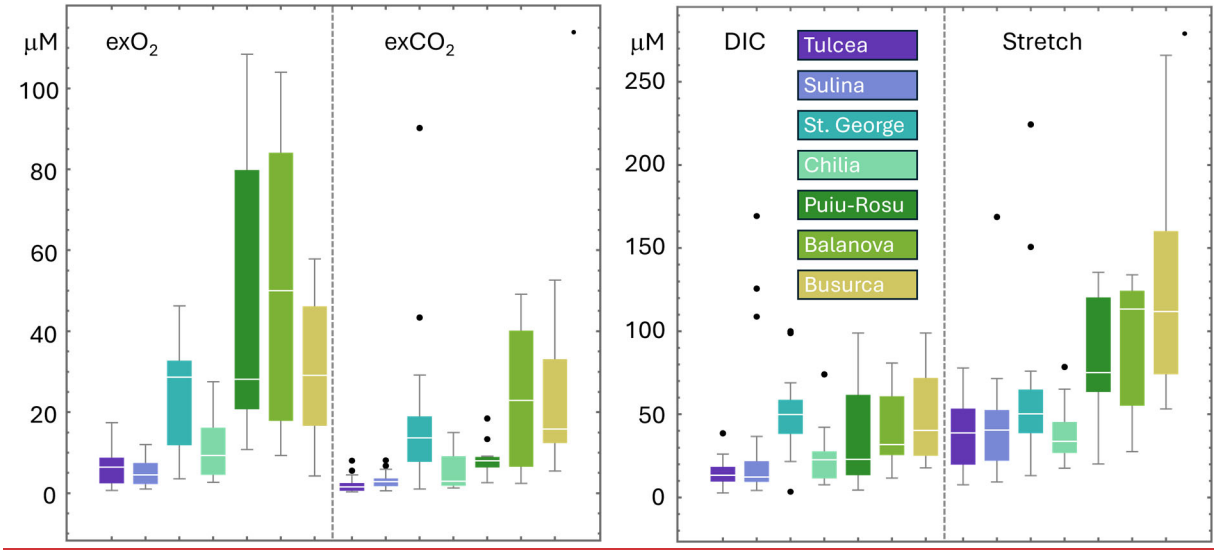

Figure 4. *Box plots of monthly mean 24-h amplitudes of exO_2, $exCO_2$, DIC and the stretch parameter. Stations from left to right: Tulcea, Sulina and St. George (2016-2017), Chilia in 2016 and Puiu-Rosu, Busurca and Balanova in 2018. The number of monthly means per station ranged from 11 to 21 (Table A1). White horizontal lines mark median values, boxes show the 25-75% quartiles and whiskers indicate the range except for outliers marked with dots.*

~~Overall Table 1 reveals two orders of magnitude difference in daily metabolic cycles between the upstream station of Tulcea in winter and the Balanova channel in summer. Averaging the annual data resulted in 6 µM $exCO_2$ and 11 µM exO_2 for the four Danube River stations and 18 $exCO_2$ and 43 µM exO_2 for the three delta stations. Compared to the river reaches, the metabolic shifts at the monthly timescale were therefore 2-2.5 times more intense within the delta water network. The average amplitudes during the warm season of April to September were about 40% larger than the annual mean values.~~

~~**Table 1.** Amplitude of average daily fluctuations (Fig. D1) in $exCO_2$ and exO_2 in µM at four Danube stations in 2016 and at three stations within the delta in 2018. The av. column shows the annual average of available data.~~

		av.	Jan	Feb	Mar	Apr	May	Jun	Jul	Aug	Sep	Oct	Nov	Dec
Tulcea	$exCO_2$	1				0.3	0.5	2	2	2	3	1	0.4	0.8
	exO_2	5				2	4	8	8	6	9	3	0.7	1
Sulina	$exCO_2$	3				3	3	7	6	2	3	3	2	1
	exO_2	4				6	6	8	6	4	2	1	1	1
St. George	$exCO_2$	15	4	8	15	17	19	29	25	12	16	8	8	
	exO_2	21	8	15	29	32	25	30	31	23	30	4	7	
Chilia	$exCO_2$	5	2	2	2	2	2	3	8	10	10	15	5	1
	exO_2	12	8	5	3	7	11	12	20	23	28	13	4	4
Balanova	$exCO_2$	24		5	2	12	25	41	37	49	48	22	23	4
	exO_2	52		9	12	35	59	95	86	104	78	50	29	14
Puiu-Rosu	$exCO_2$	8		3	3	7	8	7	14	19	8	8	6	9
	exO_2	47		11	12	28	23	68	90	108	84	50	27	20
Busurca	$exCO_2$	23		15	14	30	12	23	37	53	34	16	5	11

~~exO_2~~	~~30~~		~~13~~	~~21~~	~~42~~	~~29~~	~~47~~	~~29~~	~~58~~	~~50~~	~~21~~	~~4~~	~~15~~

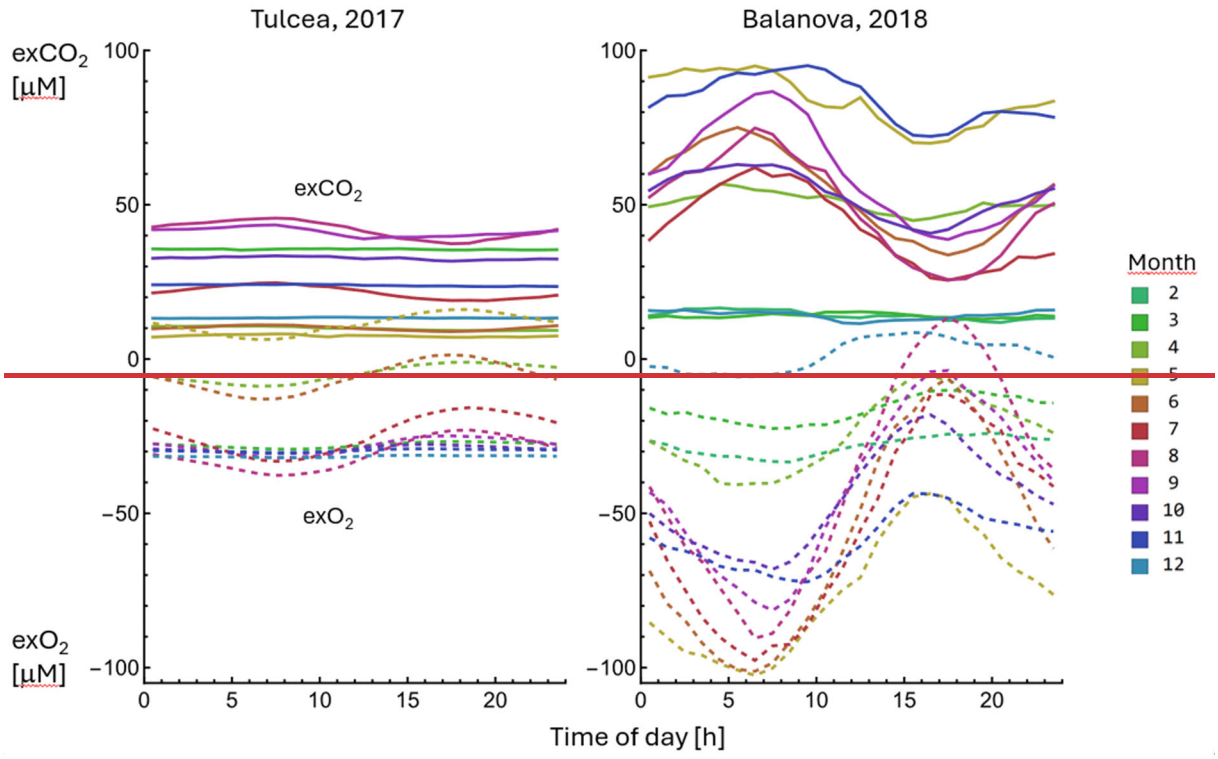

~~***Figure 3.*** *Example of 24 h monthly averages for* ***a)*** *$exCO_2$ and* ***b)*** *exO_2 at Balanova station in 2018. Time of day on x axis, excess CO_2 and O_2 on y axis, color coding shown at right. The averaged daily cycles define characteristic amplitudes and timing of river metabolism during each month. For full data see Fig. D1.*~~

~~3.2 Covariance of O_2-CO_2 dynamics~~

~~In an ideal case, aquatic photosynthesis and respiration represent the major drivers for change in dissolved O_2 and CO_2 concentrations in surface waters. A plot of exO_2 versus $exCO_2$ would then resemble a straight line with slope -1 crossing zero excess concentration (Vachon et al., 2020). At the delta stations, inflow from the wetlands and variable biogeochemical processes variability define broader domains of observed $exCO_2$-exO_2 values and associated covariance parameters (Fig. 4). We calculated covariance data from a set of 105 monthly observations (Table D1). As expected, there were strong correlations (Pearsons's $\rho > 0.5$) between the centroid CO_2 and O_2 position and the offset from the -1 line and between stretch and width, the long and short axis of the 95% ellipses (Table 2). There was weaker correlation between the centroid position and the shape parameters of the ellipses. The slope, which should relate to the ecosystem stoichiometry, showed the weakest correlations with other parameters, indicating that the intensity of river metabolism (stretch) was quite independent of the type of processes (slope).~~

~~In November 2016, the centroid coordinates at stations Tulcea, Sulina and Chilia were located close to the theoretical line in the lower right segment, i.e. in the respiratory domain of the O_2-CO_2 plot with $exCO_2 > 40$ and exO_2 around -35 µM (Fig. 4, Table D1). The over 2500 datapoints in November were confined to quite narrow covariance ellipses enclosing 95% of the datapoints measured within one month. At St. Geroge, however, the November data were spreading over a much larger area ($-50 < exCO_2 < 150$ µM, centred around enriched $exCO_2$ =102 µM and more depleted exO_2 = -47 µM). The offset of the centre is defined as the nearest distance to the 1:-~~

~~1 line and reached a value of 28 µM at St. George in November compared to a range of 4–8 µM at the other three Danube stations. This increased offset towards high CO_2 is a strong indication for lateral inflow from the reed stands in the wetland, where the decomposition of organic matter accumulates dissolved CO_2.~~

Table 2 Correlation coefficients ρ for 105 monthly parameter sets including the centroid position (c-$exCO_2$, c-exO_2), the shape parameters stretch and width, the offset, and the slope of the main ellipse axis (Data in Table D1). Bold face for $|\rho| > 0.5$ and grey font for $|\rho| < 0.2$.

parameter	c-$exCO_2$	c-exO_2	stretch	width	offset	slope
c-$exCO_2$	1					
c-exO_2	**-0.93**	1				
stretch	0.46	-0.38	1			
width	0.49	-0.45	**0.74**	1		
offset	**0.92**	**-0.75**	0.45	0.43	1	
slope	0.13	-0.14	-0.08	0.02	0.09	1

Plotting the 24-h cycles in the exO_2-$exCO_2$ plane allowed for a closer look at diel dynamics and the intensities of autotrophic versus heterotrophic ecosystem metabolism over the course of a year (Fig. 5). In the following, we focus on differences between the cold season (October – March) and the warm season (April – September). At Tulcea and Sulina, these plots illustrate minimal metabolic activity during cold months with exO_2 amplitudes in the range of 1-2 µM and comparatively small signals of 7-9 µM during the warm months. In contrast, Chilia and St. George, were characterized by significantly stronger daily cycles with mean warm season exO_2 values of 17 µM and 32 µM, respectively.

The delta stations reveal different types of dominant metabolic activities and a broad dynamic range of O_2 and CO_2. At the lake-outlet of Puiu-Rosu, autotrophic activity significantly exceeded heterotrophic metabolism with a pronounced buildup of dissolved oxygen and positive daytime exO_2 values during the warm season. In contrast, the wetland discharge defining the water characteristics at Busurca was dominated by heterotrophic signatures with extremely high $exCO_2$ concentrations of 300 – 500 µM during the warm season, while exO_2 oscillated between -150 and -250 µM and approached anoxic conditions. Balanova, showed an intermediate signature between the lake and wetland waters with warm-season exO_2-values ranging between 0 and -100 µM.

At high CO_2 supersaturation observed for instance at Busurca, Balanova and St. George, the slopes of linear regression lines often converged towards idealized values of -1 for the O_2:CO_2 stoichiometry of photosynthesis and respiration (Fig. 5). At Puiu-Rosu, however, steeper slopes were observed due to the buffer effect of the carbonate system when CO_2 values approach atmospheric equilibrium (Shangguan et al., 2025). The Busurca data followed a heuristically trajectory along a slope of -0.5, pointing extending towards $exO_2 \approx$ = –200 µM, and

$exCO_2$ ≈= +400 µM.

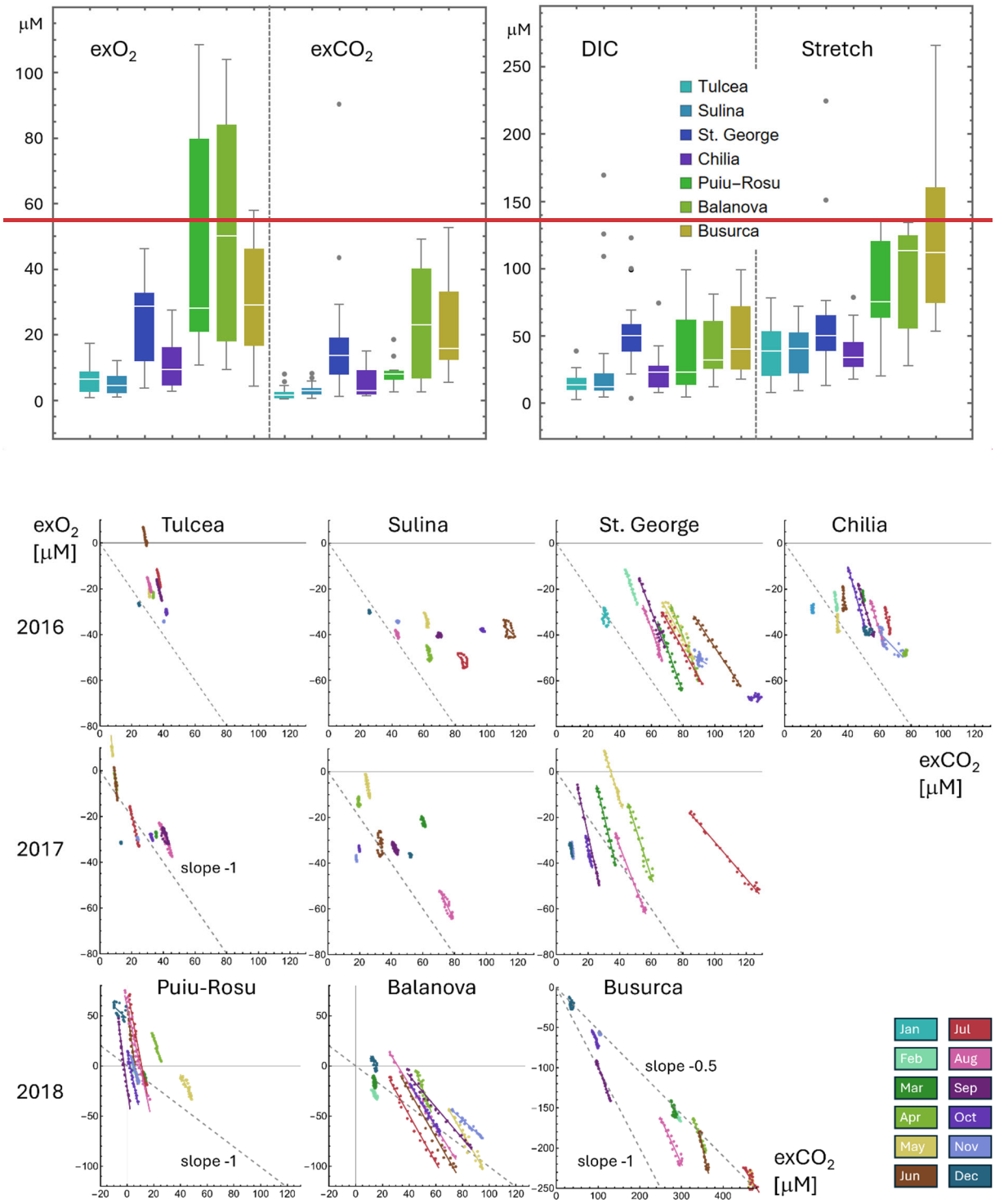

Figure 5. *Paired exO_2-$exCO_2$ plots of mean 24-h cycles. Dots represent monthly averages at one hour resolution and are connected by linear regression lines. Diagonals mark theoretical O_2-CO_2 stoichiometry of photosynthesis and respiration. Note extended x-y scale at Busurca.*

To assess the effect of potential drivers for the intensity of river metabolism such as temperature and cloud cover, we related the daily stretch parameters with mean water temperature measured by the in-situ probes and the mean daily cloud cover observed at Tulcea Airport (Table 1). Cloud cover blocking sunlight was negatively correlated

to the diel stretch parameters for the seven analysed time series. The Pearson's coefficients ρ ranged from -0.26 at Busurca to -0.46 at Chilia. On average, the cloud-cover sensitivity of the stretch factor was ~3 times larger at the delta stations compared to the river sections. The R^2 values were typically < 0.2, but the correlations were significant at the $p < 0.05$ level.

Water temperature has been identified as a key variable for respiration rates in streams (Perkins et al., 2012). In this study, the correlation between the stretch parameters and mean daily water temperatures was rather strong (range $0.37 < \rho < 0.77$) and significant ($p < 0.05$) for the seven stations (Table 1). On average, increasing water temperature enhanced the indicator of metabolic activity by 0.7 µM/°C at the river stations and by 2.8 µM/°C within the delta. For a seasonal shift in water temperature of 20°C, the corresponding change in the stretch parameter amounted to 14 and 56 µM for typical Danube River reaches and delta channels, respectively. This factor 4 difference in the temperature-sensitivity of the daily stretch parameter between river and delta sites mirrors the metabolic response to cloud cover and is in line with the higher metabolic amplitudes in the delta.

Table 1. Linear regression slopes of daily stretch values as a function of mean cloud cover at Tulcea Airport and local water temperature. R^2 is the coefficient of determination, ρ is Pearson's correlation coefficient.

		Stretch versus cloud cover			Stretch versus water temperature		
Location	**Years**	**Slope [µM/%]**	**R^2**	**ρ**	**Slope [µM/°C]**	**R^2**	**ρ**
Tulcea	2016, 2017	-0.09	0.15	-0.38	0.59	0.37	0.61
Sulina	2016, 2018	-0.07	0.04	-0.30	0.36	0.15	0.38
St. George	2016, 2018	-0.24	0.09	-0.29	1.20	0.17	0.41
Chilia	2016	-0.16	0.22	-0.46	0.80	0.48	0.69
Puiu-Rosu	2018	-0.58	0.18	-0.43	3.25	0.48	0.69
Balanova	2018	-0.47	0.12	-0.34	3.84	0.59	0.77
Busurca	2018	-0.20	0.04	-0.21	1.44	0.13	0.37

3.2. Wetland discharge

To estimate the influence of wetland discharge on the O_2-CO_2 dynamics of the Danube River along passage through the delta, we performed monthly covariance analyses exemplified by a comparison between June and November (Fig. 6). Data from the seven stations revealed significant differences in the stretch (elongation) of the 95% covariance ellipses. In November, data from the river reaches were enclosed by rather circular shapes with minimal offset from the 1:1 diagonal. The June records, however, resulted in elongated ellipses characteristic for higher amplitudes. The data patterns within the covariance ellipses formed distinct monthly fingerprints which were only slightly distorted after moving from Tulcea to the downstream stations of Sulina and Chilia but appeared randomized at St. George.

The delta stations showed smaller seasonal differences in stretch between June and November but marked shifts in the position within the exO_2-$exCO_2$ diagram. While the Puiu-Rosu data indicated intense photosynthesis with O_2 supersaturation and equilibrium-level CO_2, Busurca represented an extreme case of wetland discharge from the surrounding reed stands with CO_2-rich and O_2-depleted water masses. Balanova located downstream of Puiu-Rosu reflected a mixture of lake- and wetland water. Its monthly fingerprints resembled those of Puiu-Rosu but with a downward shift along the theoretical line of slope -1.

In the downstream Danube River reaches, wetland discharge led to increasing offsets and a shift along the heuristic slope -0.5 (Busurca, Fig 5).~~In the covariance data from June 2016, the inflow of water from the Delta wetlands is leaving its marks in all three downstream stations of the Danube (Fig. 4). The covariance ellipses show an elongated shape due to more intense photosynthesis and respiration compared to November, but the quite uniform distribution of measurements within the ellipses at St. George and Chilia corresponds to strong day night shifts, while the "random walk" of datapoints in the $exCO_2$-exO_2 domain of Tulcea and Sulina in Fig. 4 corresponds to significantly smaller amplitudes of the daily fluctuations (Table 1). Note that the oxygen dynamics at Tulcea was centred around atmospheric equilibrium in June, but in the context of the full year, this represents an exception. Usually, Tulcea waters showed slight oxygen deficits.~~ Centroids were displaced towards O_2 undersaturation by -40 µM and CO_2 supersaturation of + 35 to + 85 µM~~-~~. While offsets in June remained similar between Tulcea and Chilia, the two other downstream stations showed offset increases of 21 and 16 µM at Sulina and St. George, respectively. In November, covariance clouds remained compact and close to the -1:1 line except for St. George

where the offset exceeded that of Tulcea by more than 20 µM. Overall, these examples from two contrasting months provide clear evidence of wetland discharge affecting dissolved gas dynamics between Tulcea and the stations near the Black Sea coast.

~~The observations within the Danube Delta in 2018 reveal a striking difference to the main reaches of the Danube: In June, the covariance in the CO_2–O_2 plain is constrained by narrow 95% ellipses and the three sites widely differ in the slope of the main axis of −1.6, −7.8 and −0.3, for Balanova, Puiu-Rosu and Busurca, respectively. This contrast and the distinctive average exO_2 values (−58, +19, −206 µM) at these three sites point towards different governing processes (Table D1). Compared to the covariance analyses in the main stem of the Danube, the two sites at Balanova and Puiu-Rosu exhibit only negligible offsets while Busurca's offset in June with > 100 µM marks only one of several excursions towards high $exCO_2$ at that site. The Puiu-Rosu station seems therefore to be dominated by aquatic processes characteristics for lakes, whereas Busurca and Balanova, which collect the outflow from the wetlands, show a mixture of both sources.~~

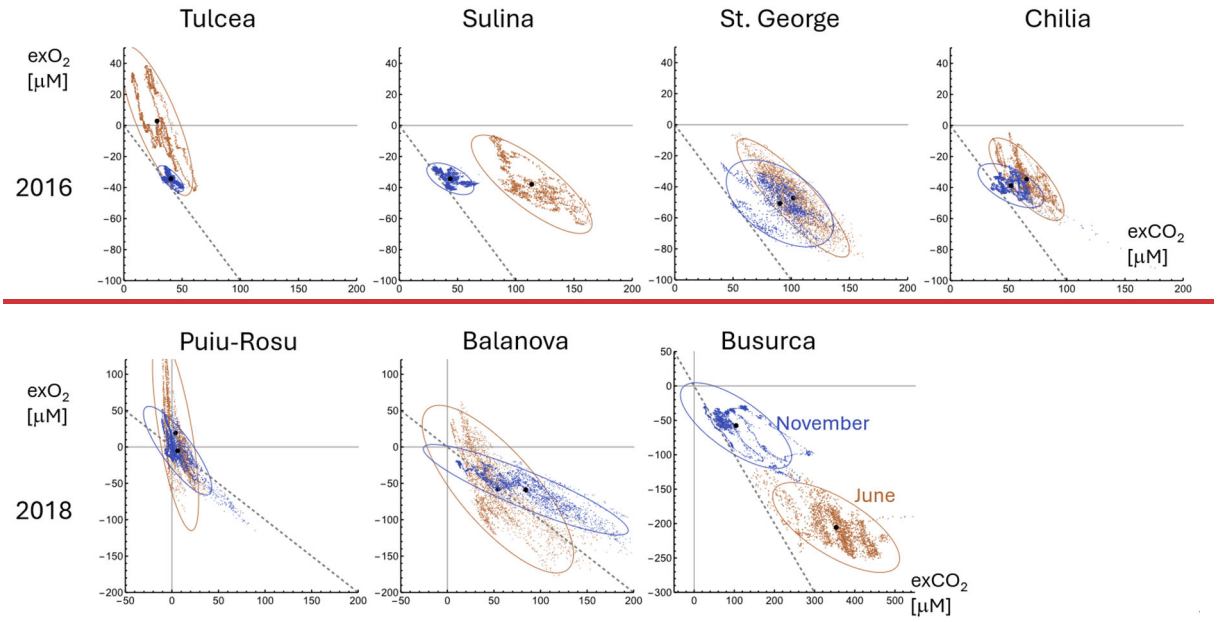

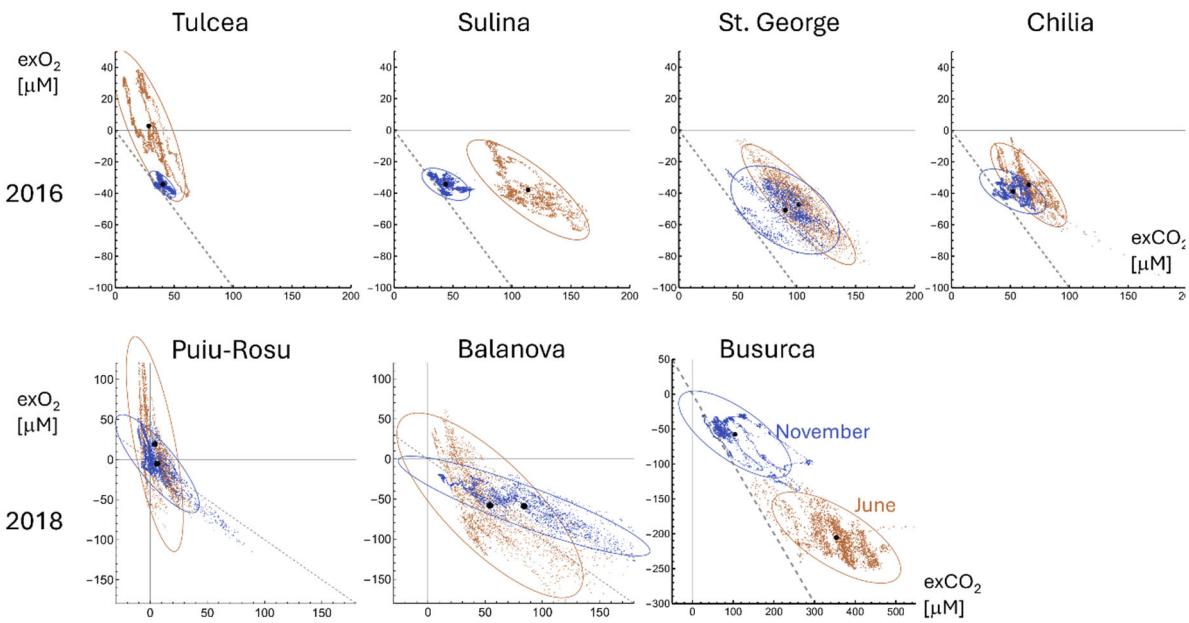

Figure 46. *Examples of covariance ellipses for exO_2 v.s. $exCO_2$ covering 95% of measured data pairs at 95% confidence level for the Danube River reaches (upper panels) and stations within the delta (lower panels). The dDiagonal lines represents the theoretical slope of -1 for photosynthesis and respiration of -1 crossing the origin. . Dots mark the centroids. Top: months June (red) and November 2016 (blue) for the four Danube River stations. Bottom: June (red) and November 2018 (blue) at stations within the delta, the Balanova station, the outflow from Lake Puiu and the station Busurca at the channel collecting outflow from the reed stands.Expanded axes for Busurca.*

4. Discussion

4.1 Lateral inflow from wetlands

In the absence of lateral inflow, one would expect very similar chemical characteristics among the Danube stations of Tulcea upstream of the Delta and the three sites of St. George, Sulina and Chilia close to the Black Sea. The data clouds, however, revealed clear differences in exO_2-$exCO_2$ between Tulcea and the stations downstream (Fig. 4). A more systematic analysis of the centroids allows tracking how the monthly means of exO_2-$exCO_2$ move evolved overover time. The results reveal quite diversedistinct annual journeys at the four Danube stations in 2016 and 2017 (Fig. 57). The trajectories at Tulcea were confined to a quite narrow quadrant between 0 and ± 40 µM for both exO_2 and $exCO_2$. At the downstream stations, however, the warm-season centroids for summer and autumn typically fall outside this range because waters were loaded with excess CO_2 andwere typically more depleted in O_2 and enriched in CO_2 compared to Tulcea. The trajectories often moved along a heuristic slope of -0.5 for wetland discharge (Busurca, Fig. 7). The increase in average $exCO_2$ between Tulcea and a downstream stations reached factors as high as of 4 (June 2016, Sulina) and 18 (June 2017, St. George). In contrast, Both stations were influenced by canals draining the delta and therefore partially reflect mixing of Danube waters with lateral inflows from the wetlands and their groundwater. Recently (Deirmendjian and Abril, 2018) reported such groundwater hotspots in first-order streams. Tthe downstream depletion of exO_2 at Sulina and St. George was less

pronounced than the $exCO_2$ loading and maximum exO_2-differences compared to Tulcea were limited to ~~a~~ factors of ~ 3 (Sulina, July 2017) and 2 (St. George, Oct. 2016). ~~In streams, the mineralization of organic matter changes dissolved CO_2 and O_2 with a 1:1 stoichiometry, but in groundwaters and wetland outflows the oxygen can be depleted to near zero concentrations, while the accumulation of dissolved CO_2 continues by anaerobic processes and may reach very high levels (Maier et al., 2022). The different hydrographs in 2016 and 2017 lead to distinct excursions in CO_2 loads at Sulina and St. George. While the recession of the spring flood coincided with an input of $exCO_2$ in June at the Tulcea branch, the very low water levels in summer 2017 (Fig. 1a) drained $exCO_2$ rich water specifically into the St. George Branch (Fig. 5). By contrast, the~~The Chilia station~~,~~ also ~~mostly recorded Danube water signatures and~~ showed consistently lower exO_2 and higher $exCO_2$ values compared to Tulcea, but ~~only moderate deviations from the centroid dynamics at Tulcea.~~extreme additions of CO_2 rich waters were not observed in this more natural river reach which remains less affected by dredged channels.

Flood dynamics appear to play an important role at the stations within the delta. ~~T~~The largest flood peak ~~in~~ during the three years of our study occurred in early April 2018 (Fig 1) and~~. It~~ was followed by a strong flood recession until mid-June. All three delta stations ~~in the Delta~~ showed the highest CO_2 loads ~~and~~ with the lowest O_2 levels in May 2018, when the flooded reed stands were likely exporting carbon-rich water into the adjacent channels and lakes. Higher discharge in July-August ~~lead to a reversed~~reversed the situation and moved the Busurca centroids towards photosynthesis-respiration line with slope -1.~~,~~ ~~but then~~However, when exceptionally dry conditions re-established the wetland discharge in October-November, ~~kicked in and even the Busurca Channel seemed to be carrying mostly Danube water in December 2018~~the Busurca centroids moved back towards the slope -0.5 line (Fig. ~~5~~7). ~~Within the delta, the Balanova station in 2018 provides an illustrative example of in-stream metabolism dominated by mineralization of organic matter generated in the wetlands of the delta (Maier et al., 2022). During summer, the centroids remained in the domain of oxygen deficits but follow the 1: 1 stoichiometry quite closely (Fig. 5). The Busurca Channel, however, represents an endmember collecting mainly waters from the wetland, with a pattern strongly deviating from the stoichiometry of river metabolism and average oxygen levels approaching anoxic conditions with close to ~ 250 µM exO_2 in spring and summer and dissolved CO_2 concentrations exceeding a 30-fold oversaturation (470 µM $exCO_2$) in May and June. Such a water composition of almost 500 µM $exCO_2$ could be defined as an observed endmember in the water composition of the wetlands. In such a scenario, maximum excursions with maximum offsets of 20 µM at Chilia (June 2016), 54 µM in Sulina (June 2016) and of 116 µM at St. George (June 2017, Table D1) would correspond to mixtures of Danube water with ~ 4, ~ 10 and ~ 25% CO_2 rich wetland water, respectively.~~

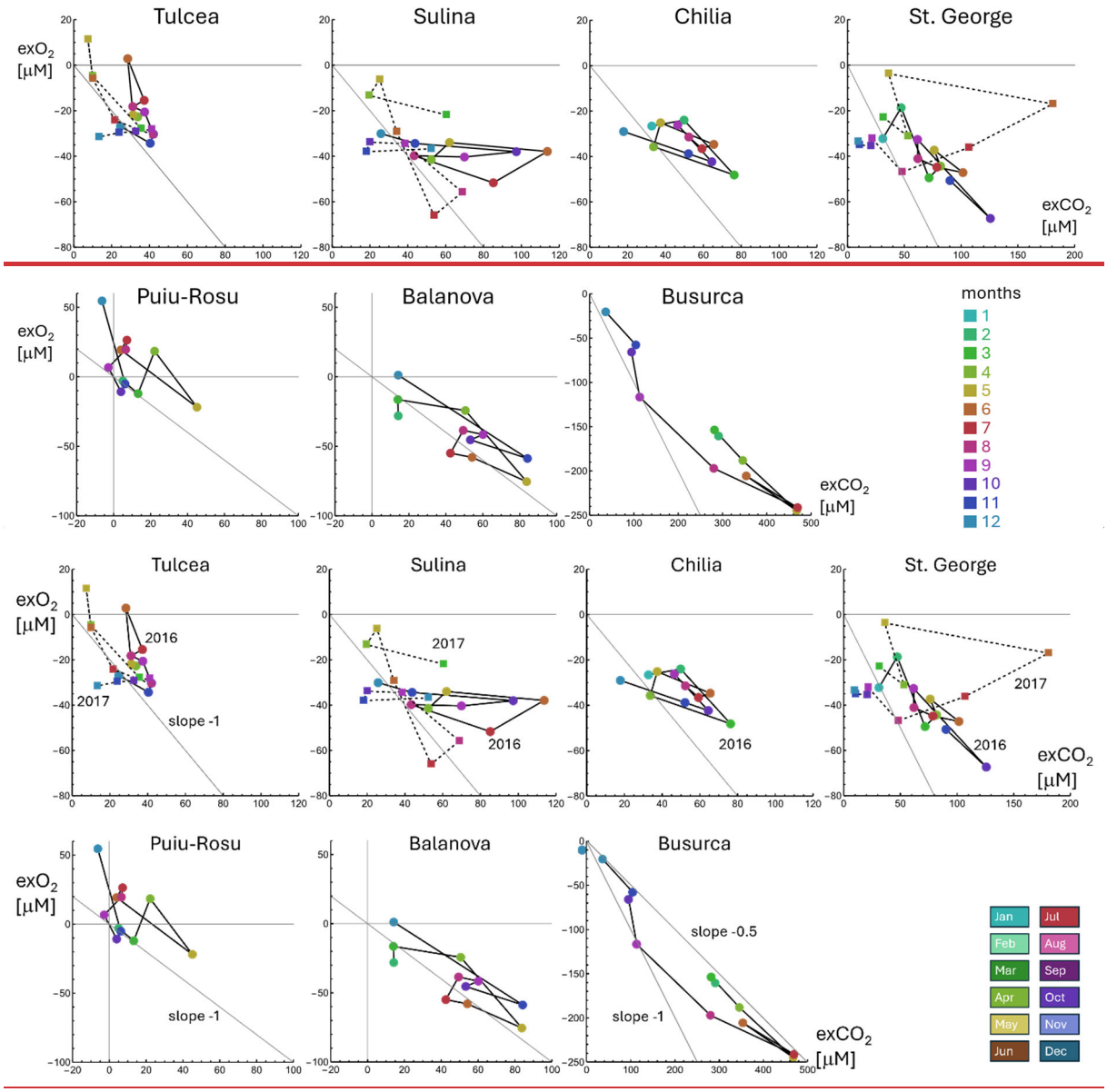

Figure ~~5~~7. *Top: Annual trajectories of monthly centroids at the four Danube River stations ~~in 2016 (dots connected by solid lines) and 2017 (squares connected by dotted lines~~ in 2016 and 2017~~)~~. ~~Note different~~ Extended x-axis for St. George. Bottom: Monthly centroids at three stations within the Danube Delta in 2018. ~~(dots with black lines). Note different~~ Extended x-y axes for Busurca.*

3.3. CO_2 emissions

To compare CO_2 emission rates across the delta, we calculated average $exCO_2$ values at the seven stations. To avoid sampling bias caused by interruptions during winter, we interpolated missing months by average cold season values and obtained mean emission rates over two years for Tulcea, Sulina and St. George and over one year for the other stations (Table 2). The average $exCO_2$ at the three downstream stations was 54 µM corresponding to a 1.9 times higher supersaturation level than at Tulcea.

In 2018 the lake outflow at Puiu-Rosu showed only 31% of the $exCO_2$ supersaturation observed at Tulcea in the two preceding years, whereas the wetland discharge at Busurca reached almost an order of magnitude higher

$exCO_2$ levels. In a previous study based on discrete samples and floating chamber measurements, Maier et al. (2021) determined the median values of the gas transfer coefficients k_{600} [m s^{-1}] for the different waterscapes of river reaches, lakes and channels. These results allowed the estimation of updated CO_2 emission rates based on the

Table 2 *Average $exCO_2$ supersaturation recorded in 2016-2017 at Tulcea, Sulina and St. George, in 2016 at Chilia and in 2018 at Puiu-Rosu, Balanova and Busurca. Warm = warm season, Apr.- Sep., cold = cold season, Oct.-Mar.*

Station	Tulcea	Sulina	St. George	Chilia	Puiu-Rosu	Balanova	Busurca
av. $exCO_2$ [µM]	29	51	62	49	9	46	250
Ratio Station/Tulcea	1	1.8	2.1	1.7	0.3	1.6	8.6
av. $exCO_2$ [µM] warm	28	57	76	49	14	57	340
av. $exCO_2$ [µM] cold	30	45	49	49	4	36	160
Ratio warm/cold	0.9	1.3	1.6	1.0	3.1	1.6	2.1

continuous sensor observations. For the river reaches, we assumed an emission scenario of a linear increasing between Tulcea and the three downstream stations. For comparison with an earlier study (Maier et al., 2021), the Puiu-Rosu station was used as representative estimate for lakes and the average between Balanova and Busurca was assumed to represent the mean channel emission rate (Table 3).

Despite substantially higher CO_2 concentration in channels compared to the river reaches and lakes, the waterways of the delta contribute a similar amount as lakes to total emissions because of their small surface area. According to data from global meta-analyses, the vast area of reed stands holds the potential for significant CO_2 drawdown (Li et al., 2025; Lu et al., 2017).

Table 3 *CO_2 emission rates across aquatic ecosystems in the Danube Delta based on average $exCO_2$ values and median gas transfer rates. The 25 and 75% quartiles are shown in brackets. Gg = 10^9 g*

Ecosystem	River reaches	Lakes	Channels	Reed stands
Average $exCO_2$ [µM]	42	9	148	
k_{600} [m d^{-1}] *	0.69 (0.49-1.12)	1.2 (0.72-1.80)	0.74 (0.44-1.27)	
Area [km^2] *	164	258	33	1600
CO_2 emission [mmol m^{-2} d^{-1}]	29 (20-47)	11 (7-16)	110 (65-190)	
CO_2 emission [Gg C yr^{-1}]	21 (15-33)	12 (7-18)	16 (9-27)	
CO_2 emission [Gg C yr^{-1}] *	22	19	19	
CO_2 uptake [Gg C yr^{-1}] **				270-330

** Data from Maier et al. (2021), ** estimated from Li et al. 2025 and Lu et al. 2017*

4. ~~(Li et al., 2025; Lu et al., 2017)~~Discussion

4.1 Variability of ecosystem metabolism

Why is it relevant to study the differences in river metabolism between lowland river reaches and wetland channels? Over the last century between 70 and 80% of wetlands have been drained mostly for agriculture in the major countries of the Danube basin while at the same time the nitrogen surplus from fertilized cropland has

increased threefold (Bertassello et al., 2025). Restoring riparian wetlands within the Lower Danube Green Corridor (Csagoly et al., 2018) is now an established policy goal for improving flood protection, removing excess nitrogen (Tschikof et al., 2022) and potentially sequestering carbon (Hemes et al., 2018). In the context of assessing the biogeochemical effects of floodplain restoration, the Danube Delta provides a unique opportunity to characterize the aquatic system metabolism of large river reaches and connected wetland channels side by side.

Our study provides evidence for significantly faster metabolic processes in the slowly moving waters of the delta wetlands compared to the main river reaches of the Danube. The monthly averages of 24-h amplitudes and the stretch of exO_2-$exCO_2$ covariance ellipses consistently indicate a 4-8 times more intense aquatic ecosystem metabolism within the delta. Additional analyses of daily DIC variability support this result, although the DIC patterns exhibit higher stochasticity due to hydrological fluctuations. In contrast the direct response of O_2 to photosynthesis and respiration, DIC concentrations are influenced by a broader range of interacting processes, like groundwater inputs, sediment-water exchange, and episodic flooding events. These hydrological perturbations can alter both the concentration and residence time of dissolved carbon, partially masking the metabolic signal at daily time scales.

The mean daily exO_2 amplitude as an indicator for metabolic activity covered two orders of magnitude from cold season values in the upstream station of the Danube with cold-season values around 1 µM at Tulcea to a warm season maximum of 100 µM observed at Balanova station in August 2018. The dense aquatic vegetation in the delta lakes and channels including floating reed, riparian vegetation, macrophytes and high chlorophyll concentration translate into high substrate availability for ecosystem respiration (Coops et al., 2008; Oprea et al., 2024). A hydrological model for the Delta estimated travel times across the network of channels and lakes on the order of 2-3 weeks for the Puiu-Rosu and Balanova stations (Oosterberg et al., 2000), facilitating a high biomass concentration in prolonged contact with moving water. Average $exCO_2$ concentrations close to 0.5 mM at Busurca in May and July 2018 may therefore result from the accumulation of mineralization products over timespans of weeks in water parcels traversing the reed stands (Fig 5). By contrast, water residence times in the main river reaches are much shorter: sensor data revealed travel times between Tulcea and in the three downstream stations on the order of one day for Sulina and St. George and two days for Chilia essentially limiting the time for accumulating changes in O_2 and CO_2. ~~(Tiegs et al., 2019)~~

The significant differences between the three river reaches, can likely be attributed to their morphology and hydrological connectivity. Patterns exO_2-$exCO_2$ pairs within covariance ellipses retained close similarity between Tulcea and the downstream stations of Sulina and Chilia, whereas they appeared “randomized” at St. George (Fig. 6). The Sulina channel has been strongly modified for navigation with straight geometry and dykes that reduce lateral exchange, while the Chilia branch retains a more natural meandering geometry. The St. George reach consist of natural meanders and straight cuts for navigation, resulting in a broader distribution of water travel times and more intense exchange with adjacent wetlands and aquifers. This close interaction with wetlands at St. George likely superimposes multiple water masses with different metabolic histories, thereby disrupting the coherent diel covariance patterns that were preserved at Sulina and Chilia. Consequently, the 24-h amplitudes of exO_2, $exCO_2$ and DIC all follow the sequence St. George > Chilia > Sulina consistent with decreasing lateral connectivity (Fig. 4).

We used the daily stretch factors to test hypotheses that water temperature and cloud cover would influence the intensity of aquatic metabolism (Table 1). Overall, the correlation between cloud cover and covariance stretch was weaker than for water temperature as a forcing factor. The relations between cloud cover, photosynthetically active

radiation, PAR, (Kathilankal et al., 2014) and metabolic response are inherently complex in multiyear (Dodds et al., 2013) or multisite analyses (Mulholland et al., 2001). As cloud cover does not directly translate to in-situ light conditions due factors like the seasonality of daylight and water transparency, further assessments require local PAR analyses at the monitoring stations. Such local data were available for determining the temperature sensitivity of metabolic amplitudes. The regression of daily mean in-situ temperatures with diel stretch factors resulted in a temperature sensitivity of the aquatic metabolism of 0.7 µM/°C in river reaches and 2.8 µM/°C in delta channels. These results suggest that a warming climate would affect the wetland's aquatic metabolism about four times more strongly than main river branches. Previous studies have shown that biofilm respiration exhibits complex temperature sensitivity (Dybdahl et al., 2024) while ecosystems with higher quantities of organic substrate are subject to stronger temperature sensitivity of ecosystem respiration (Jankowski et al., 2014).

The timing of daily cycles indicates a preferred sampling window around noon for obtaining representative values of O_2, CO_2 and DIC, whereas the early hours of 5-8 am and the late afternoon of 3-6 pm would introduce the largest sampling biases in the case of the lower Danube aquatic ecosystems (Fig. 3, Fig D1). For logistical reasons, field work is often scheduled between the late morning and early afternoon hours, which likely explains, why the CO_2 emission rates based the continuous monitoring of this study (Table 3) agrees very with results from grab samples collected during field campaigns during the same years (Maier et al., 2021).

4.2 Wetland discharge

What are the effects of wetland discharge on river biogeochemistry and how can we identify its origin and magnitude? Large-scale approaches may analyse the CO_2 dynamics within an entire river system~~(Borges et al., 2019; Abril and Borges, 2019)~~: sampling transects across the Congo River a study demonstrated that lateral connectivity with riparian wetlands was driving spatial and temporal variability of CO_2 concentrations and the river's greenhouse gas emissions (Borges et al., 2019). More targeted study designs focus directly on wetland drainage pathways: recent studies revealed disproportionally high contributions of ditches to CO_2 emissions from Dutch peatlands (Van Der Knaap et al., 2025) and from a *Phragmites* dominated Chinese wetland (Xue et al., 2025). In the present study, we combined both approaches, although logistical constraints prevented synchronous observations of river reaches and delta channels.

The order of magnitude of $exCO_2$ found in the delta channels compares well with a global meta-analysis of wetland ecosystem metabolism (Richardson et al., 2024). These authors reported mean v~~(Richardson et al., 2024)~~alues of dissolved pCO_2 for fens and bogs of 3400 and 4100 ppm, respectively, which corresponds to approximately 100 µM $exCO_2$ and falls within the range of downstream Danube stations with $exCO_2$ of ~50 µM and the extreme case of Busurca with 500 µM (Fig 7). The mixing ration of wetland discharge in the Danube branches can be estimated based on the mean warm-season offset at Busurca (~ 100 µM). If we interpret offsets of 0 – 100 µM as a proxy for lateral inflow of 0-100%, then the warm-season offsets observed in 2016 at Chilia, Sulina, and St. George would correspond to contributions of wetland discharge of 13, 22 and 25% to total flow in these River reaches. These estimates should be considered as upper limits considering that the diversion of Danube water through the delta was estimated at 10% (Oosterberg et al., 2000). The discrepancy can be attributed to incomplete horizontal mixing, and the positioning of the sensors close to the riverbanks. At the St. George station the inflow from the Tartaru Channel probably contributed the large offsets observed between May and July 2017 (Fig 7).

A quantitative assessment of the different lateral interactions affecting the three Danube River reaches was based on monitoring the average monthly difference in DIC concentrations between the downstream stations and the

inflow at Tulcea (Fig. C3). Integrating these differences from April to December 2016 reveals an annual DIC addition of 0.5 and 1.2 mol m^{-3} yr^{-1} at Sulina and St. George, respectively. The observations in 2017 provided a similar result for St. George, but a higher accumulation rate for the Sulina stations. The seasonal balance for the Chilia branch, however, resulted in a negative value (-0.1 mol m^{-3} yr^{-1}). These contrasting observations can be explained by differences in hydrological connectivity and the origin of lateral inflows. Sulina and St. George are receiving carbon-rich wetland water. The important northern inflow to Chilia, however, originates from Lake Yuluph, the largest freshwater lake in Ukraine. Water from this system is transported via Lake Kuhurlui and connecting channels to the Chilia branch and appears to deliver DIC-depleted water.

A final question remains: how can we explain the unusual stoichiometry of up to -1:2 for exO_2:$exCO_2$ during the warm season at the station downstream of the delta and within the Balanova and Busurca channels receiving wetland discharge? A mapping campaign in October 2017 with in-situ CH_4 sensors ~~(Canning et al., 2021)~~reported median CH_4 concentrations of 0.54, 0.70 and 2.2 µM for the Danube reaches, lakes and channels and an extreme value of 16 µM at a hotspot site near Busurca station (Canning et al., 2021). These data provide indirect evidence for an important source of CO_2 co-generated by methanogens in anaerobic sediments of the reed stands. This anaerobically generated CO_2 contributes to the offset towards a diagonal of slope -0.5 (Fig 7). A portable membrane inlet mass spectrometer for O_2, N_2, He and Ar used during the same campaign in May and October 2017 revealed additional processes affecting O_2:CO_2 ratios including excess air formation in riverbanks and root ventilation in Phragmites stands. These processes may fuel methane oxidation but will remain "invisible" to sensors in the water column (Maier et al., 2022). Therefore, anaerobically generated CO_2 accumulating in the water column of reed beds, provided a distinct biogeochemical signature for identifying wetland discharge to channels and river reaches in the delta.

4.3 CO_2 emissions by the wetland pump

In their perspective paper, Abril and Borges (2019) ~~(Abril and Borges, 2019)~~argued that riparian wetlands should be included in an expanded version of the reactive pipe concept for rivers (Cole et al., 2007). With their high productivity and slow gas-exchange at the air-water interface, riparian wetlands release large amounts of dissolved CO_2. Additional fluxes of plant litter, and DOC add to the function of wetland discharge as a carbon pump. There is now increasing evidence that the wetland CO_2 pump is increasing CO_2 emissions of inland waters across different climatic zones from the tropical Congo River (Borges et al., 2019) to the arctic River Ob (Vorobyev et al., 2024).

The $exCO_2$ records (Fig. 5, Table 2) allow constraining magnitude and timing of the wetland pump in the Danube Delta. Overall, the downstream stations exhibited $exCO_2$ values which were 1.7 to 2.1 times higher than measured at Tulcea. Within the delta the high productivity of the Lake Puiu-Rosu complex reduced the average CO_2 supersaturation to 30% with reference to the inflowing Danube water indicating substantial CO_2 uptake. In contrast, wetland discharge increased the average $exCO_2$ by factors of 1.6 and 8.6 at Balanova and Busurca. The excess CO_2 levels remained relatively constant at Tulcea and in the near natural Chilia branch receiving mainly lake outflow. Within the delta channels and at the Sulina and St. George stations, however, the wetland pump was most active during the warm season with $exCO_2$ ratios between the warm and cold season of 1.3 – 2.1 (Table 2). This pronounced seasonality of the carbon pump is likely driven by the significant temperature dependence of the aquatic metabolism (Table 1) and the hydrological dynamics with flood peaks in spring an early summer (Fig 1a).

The day-night cycles of $exCO_2$ reached their maximum typically in the morning hours and showed a minim in the late afternoon and early evening (Fig. 3). Individual water samples were taken across the delta in 2016 and 2017 during daytime (Maier et al., 2021). The analysis of the three river reaches revealed no significant difference between individual water samples and the average values from the high-frequency records in this study (Table 3). This result seems to contradict a global study (Gomez-Gener et al., 2021) which reported evidence for higher night-time CO_2 emissions from rivers based on an extensive compilation of day and night CO_2 data. Analysing the 24-h cycles at the four Danube River stations in more detail (Fig. D1) reveals that sampling around midday captured values relatively close to mean daily conditions because $exCO_2$ maxima and minima were cantered around the early morning and late afternoon hours, respectively. For systems affected by the wetland pump, these results indicate that the day-night sampling bias will depend on factors like lateral connectivity and water exchange rates.

Finally, we must address the "elephant in the delta" – namely the role of CO_2 uptake by wetland vegetation and specifically by *Phragmites* stands. Direct carbon uptake by emergent wetland plants remains largely invisible to aquatic sensing, yet meta-analyses of net ecosystem production (NEP) report average global values of 168 and 208 g C m^{-2} yr^{-1} for marshes (Li et al., 2025) and coastal wetlands (Lu et al., 2017), respectively. Applied to a 1600 km^2 area of *Phragmites* dominated reed stands in the Danube Delta, these rates correspond to a carbon uptake on the order of 270-330 Gg C yr^{-1}. This estimated uptake is roughly five time higher than the diffuse CO_2 emissions from water surfaces in the delta region estimated as 49 Gg C yr^{-1} (this study, Table 3) and 60 Gg C yr^{-1} (Maier et al., 2021). This scenario estimates indicate that the wetland CO_2 pump observed in the Danube delta is driven by the highly productive wetlands which act as strong net sink for CO_2 at the landscape scale. Much of the CO_2 released into channels and river branches originates from the respiration of recently fixed organic matter within reed stands and wetland sediments. At the same time, the sustained primary production of Phragmites seasonally removes atmospheric CO_2 and transfers carbon into submerged biomass and accumulating sediments. The high CO_2 emissions from water surfaces in the delta are therefore part of an efficient carbon processing ecosystem which likely acts as a net CO_2 sink at the landscape scale.

These estimates are plausible, given that an average 10% of the Danube water passes through the delta (Bondar, 1994) and the wetland outflow near the monitoring stations of Sulina and St. George was incompletely mixed with river water.

The Puiu-Rosu station was dominated by the outflow of Lake Puiu and provides a contrasting example of average exO_2 dominated by photosynthesis and very low or even negative $exCO_2$ due to uptake by algae and macrophytes. Here, the highest CO_2 levels were observed in May which is consistent with the other two stations at Balanova and Busurca. The probable driver for inputs of CO_2-rich water was a flood recession in response to the extreme flood peak in April 2018 (Fig. 1a). During summer, the centroids of Puiu-Rosu cluster around equilibrium values of CO_2 and oversaturation with respect to atmospheric oxygen.

4.2. Flooding and flood recession

While tracking monthly centroids helps detecting lateral inflows at monthly to seasonal timescales, we need a finer time-resolution to test hypotheses regarding the drivers for lateral exchange. For this study, daily water level records at Tulcea were available as flow proxies (Fig. 1a). Therefore, we tested the hypothesis that floods would push water into the wetlands, which would then carry high CO_2 water with O_2 deficits back into the delta's channel network when water levels decreased. Time-delay analysis of peak conductivity and turbidity at Tulcea compared to the downstream stations revealed flow times of approximately 1 day from Tulcea to Sulina and 2 days to Chilia and St. George. Based on published work, we assumed typical delay times of 20 days to Puiu-Rosu and 40 days to Balanova (Oosterberg et al., 2000), but these travel times may vary and the estimates are therefore poorly constrained. We excluded three data sets with significant gaps from the analysis: Chilia 2016, Sulina 2017 and Busurca 2018.

As expected, the coefficients ρ of $exCO_2$ had opposite sign compared to exO_2, however, correlations between daily covariance parameters and time-shifted Tulcea water levels revealed some puzzling results (Table 3): the shape parameters (stretch and width) and the offset had different signs on the correlation coefficient ρ at St. George in 2016 compared to 2017. In 2016, the daily $exCO_2$ centroids were positively correlated with water levels indicating a trend that flooding was pushing CO_2-rich wetland water towards the monitoring station, while the weak negative correlation in 2017 points toward the role of flood recession in building up the large $exCO_2$ observed at minimal discharge values in June (Fig. 5). These contrasting correlations indicate that upstream daily flood levels alone cannot predict the transfer of CO_2 and O_2 from wetlands to river reaches. The timing of discharge peaks and minima in relation to the seasonal CO_2-O_2 dynamics in the wetlands seems to play a significant role in the covariance analysis of annual data.

A comparison of the correlation between offset and time-adjusted water levels in Tulcea for two time series of Puiu-Rosu and Balanova illustrates this critical relationship between aquatic metabolism and the dynamics of flooding and flood recession (Fig. 6). The lake ecosystem of Puiu-Rosu remained close to the -1 line in autumn so that the high CO_2 flood pulse in spring determined the slope of the linear regression. By contrast, the wetland dominated Balanova Channel received significant CO_2 inputs when low water levels were draining the reed stands in autumn. We can therefore reject the simple hypothesis that upstream water levels of the Danube could predict daily CO_2-O_2 dynamics within the delta. Local water level measurements are needed for a meaningful analysis. The "annual journey of centroids" in Fig. 5, however, provides a valuable basis for qualitative assessments of lateral inflows and their contributions to exO_2-$exCO_2$ dynamics at monthly to seasonal time scales.

Table 3. Daily covariance analysis of seven continuous timeseries of $exCO_2$ and exO_2 data at five stations. The data were correlated with time-adjusted water level measurements at Tulcea. The Chilia, Busurca and Tulcea 2017 results were omitted due to irregular data gaps. Bold face for $|\rho| > 0.5$ and grey font for $|\rho| < 0.2$

time series	delay [d]	c-$exCO_2$	c-exO_2	stretch	width	slope	offset
Tulcea 2016	0	-0.06	0.38	0.16	0.18	0.04	0.43
Tulcea 2017	0	-0.27	0.23	-0.29	-0.42	-0.07	0.06
Sulina 2016	1	0.17	-0.17	0.24	0.41	-0.08	0.13
St.George 2016	2	**0.55**	-0.39	0.42	0.29	0.07	0.42
St.George 2017	2	-0.15	0.40	-0.26	-0.26	-0.11	-0.02
Puiu-Rosu 2018	20	**0.58**	-0.04	-0.19	0.29	0.00	0.36
Balanova 2018	40	-0.08	-0.07	0.02	0.21	-0.08	-0.20

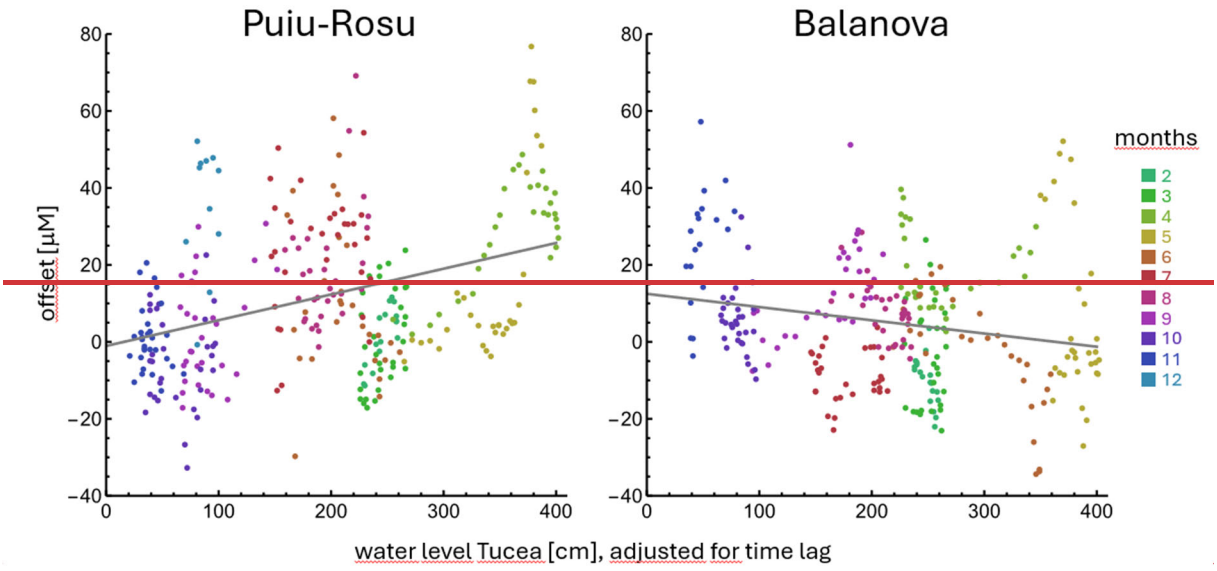

Figure 6. *Linear regression between time-adjusted Danube water levels at Tulcea and daily offset at Puiu-Rosu and Balanova in 2018. Time lag at Puiu-Rosu and Blanova was 20 and 40 days respectively.*

4.3 Intensity of river metabolism

While the annual trajectories in CO_2-O_2 space reflect the dynamics of lateral inflows, a closer look at diurnal cycles helps comparing the intensities of autotrophic versus heterotrophic ecosystem metabolism. For a quantitative analysis, we re-plotted the 24-h monthly averages at one hour resolution (Fig. 7). These graphs illustrate the minimal metabolic activity during winter months and comparatively small signals of river metabolism during the summer months for Tulcea and Sulina with some addition of wetland CO_2 downstream at Sulina. St. George and Chilia, however, were characterized by strong daily cycles in exO_2 in a background of CO_2-rich wetland water. Within the delta, Balanova represented an example of intense metabolic activity with exO_2 amplitudes up to 100 µM (Table 1). While Puiu-Rosu showed the same intensity, this lake environment represented a case where autotrophic activity significantly exceeded heterotrophic metabolism with positive values of daytime exO_2 during most of spring and summer and even undersaturation of CO_2 in September. By contrast, from April to August Busurca station is completely dominated by wetland waters and exhibited similar day-night dynamics as Balanova, but the oxygen dynamics was significantly smaller due to heterotrophic and methanotrophic activity: in May and July, Busurca station approached complete anoxia.

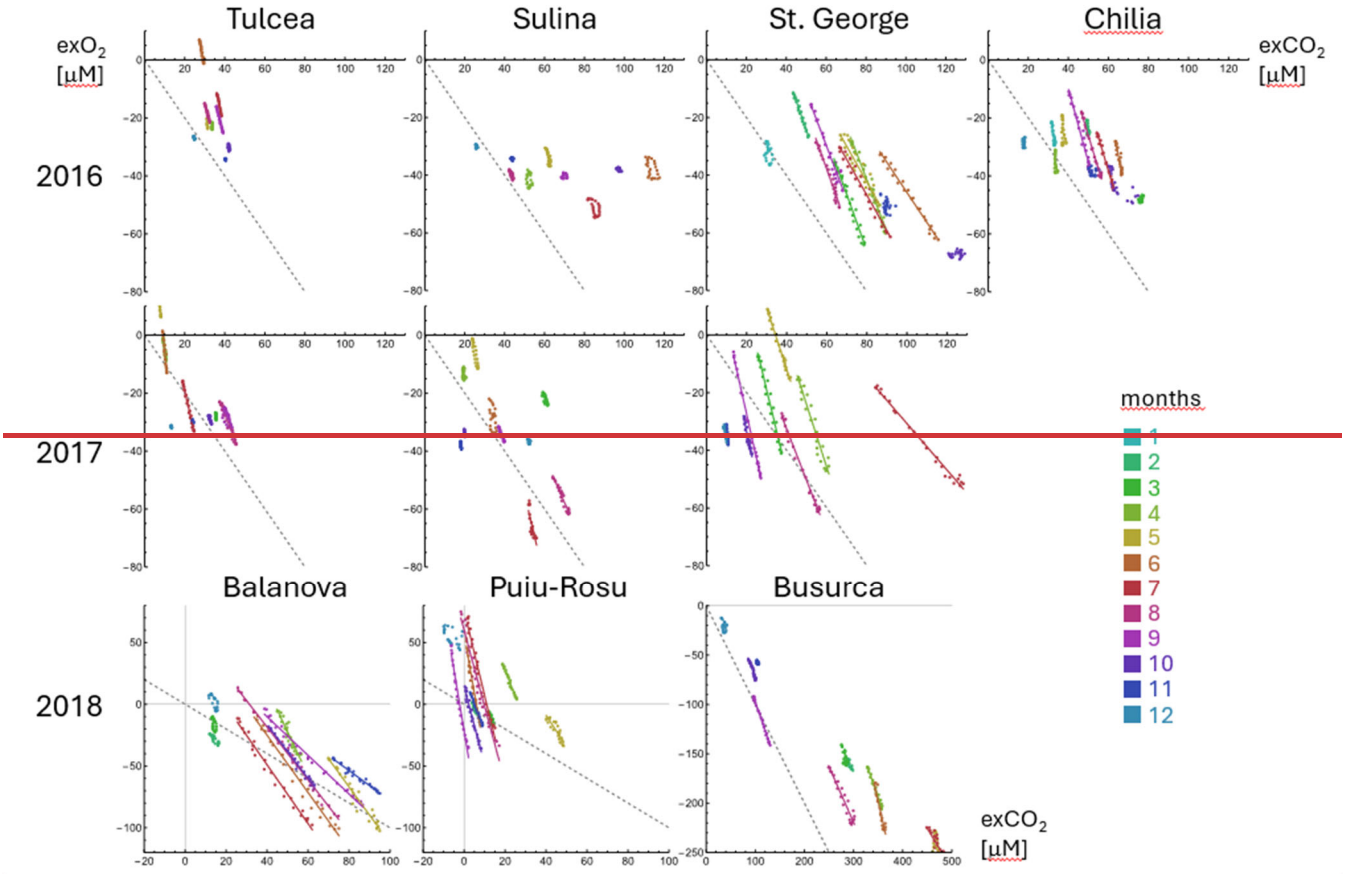

Figure 7. Paired $exCO_2$ vs exO_2 plots of monthly 24-hour cycles. Dots showing averaged measurements at one hour resolution and their regression lines are color-coded for each month. Grey dotted lines mark theoretical CO_2-O_2 stoichiometry. Same scales for the Danube stations and between Balanova and Puiu-Rosu.

To explore the effect of potential drivers for metabolic intensity at short timescales, we correlated stretch factors [µM] of the daily ex-CO_2-exO_2 cycles with daily averaged water temperature recordings from the EXO2 probes and the cloud cover observations from Tulcea airport (Table 4). As expected, there was a

~~negative correlation between average daily cloud cover blocking sunlight and the diel stretch parameters for the ten analysed annual time series. The Pearson's coefficients ρ ranged between -0.11 at Sulina in 2016 and -0.43 at Puiu-Rosu. The rather weak correlation was not surprising given the distance of > 150 km between Tulcea airport and the sampling stations. In addition, the relation between cloud cover, photosynthetically active radiation (Kathilankal et al., 2014) and metabolic response is rather complex in multiyear (Dodds et al., 2013) or multisite analyses (Mulholland et al., 2001). As cloud cover spans the range of 0 to 100%, the cloud-sensitivity of the stretch factor may explain between 7 and 58 µM of stretch variability at Tulcea and Puiu-Rosu, respectively. On average, the cloud-cover sensitivity of the stretch factor was ~4 times larger at the delta stations compared to the river sections.~~

~~As expected, water temperature has been identified as a dominant variable for respiration rates in streams (Perkins et al., 2012). In this study, the correlation between average daily water temperatures and the stretch parameters as a measure of metabolic intensity was rather strong (range $0.37 < \rho < 0.77$) for the ten annual records (Table 4). On average, increasing water temperature accelerated metabolic activity at the river stations by 0.7 µM/°C and within the delta by 2.8 µM/°C. For a seasonal shift in water temperature of 20°C the corresponding change in the stretch parameter amounted to 14 and 56 µM for typical Danube River reaches and delta channels, respectively. This four-fold difference in the temperature-sensitivity of the daily stretch parameter between river and delta mirrors the metabolic reaction to cloud cover. We may~~

~~therefore infer that the daily metabolic activity within the delta network was about a factor four more intense than in the main river reaches.~~

~~Table 4. Pearson's correlation coefficient ρ of daily stretch values and daily averages of cloud cover at Tulcea Airport and average local water temperature. Bold face for $|\rho| > 0.5$ and grey font for $|\rho| < 0.2$~~

~~time series~~		~~stretch [µM] vs. cloud cover [%]~~		~~stretch [µM] vs. water temp. [°C]~~	
~~station~~	~~year~~	~~ρ~~	~~slope [µM/ %]~~	~~ρ~~	~~slope [µM /°C]~~
~~**Tulcea**~~	~~**2016**~~	~~**-0.36**~~	~~**-0.07**~~	~~0.53~~	~~**0.40**~~
	~~**2017**~~	~~**-0.40**~~	~~**-0.10**~~	~~0.70~~	~~**0.79**~~
~~**Sulina**~~	~~**2016**~~	~~**-0.11**~~	~~**-0.02**~~	~~**0.41**~~	~~**0.31**~~
	~~**2017**~~	~~**-0.30**~~	~~**-0.07**~~	~~**0.38**~~	~~**0.36**~~
~~**St. George**~~	~~**2016**~~	~~**-0.27**~~	~~**-0.13**~~	~~**0.42**~~	~~**0.64**~~
	~~**2017**~~	~~**-0.27**~~	~~**-0.28**~~	~~**0.41**~~	~~**1.83**~~
~~**Chilia**~~	~~**2016**~~	~~**-0.29**~~	~~**-0.12**~~	~~**0.48**~~	~~**0.65**~~
~~**Balanova**~~	~~**2018**~~	~~**-0.34**~~	~~**-0.47**~~	~~0.77~~	~~**3.84**~~
~~**Puiu-Rosu**~~	~~**2018**~~	~~**-0.43**~~	~~**-0.58**~~	~~0.69~~	~~**3.25**~~
~~**Busurca**~~	~~**2018**~~	~~**-0.21**~~	~~**-0.20**~~	~~**0.37**~~	~~**1.44**~~

~~4.4 Pathways of carbon turnover~~

~~As outlined by Vachon et al. (2020), additional processes like carbonate precipitation will affect the position and slope of covariance ellipses. Based on previous regional (Maier et al., 2022) and temporal surveys (Canning et al., 2021) in the Danube Delta, we can expect significant contributions of CH_4 oxidation to O_2-CO_2 dynamics. Methanotrophic bacteria (Oswald et al., 2016) effectively compete for O_2 (Mayr et al., 2020) with microbial communities involved in the oxic respiration of organic matter (Eq. 1) in a chemoautotrophic process to oxidize CH_4 with O_2 (Eq. 2).~~

~~$$\text{“}CH_2O\text{”} + O_2 \leftrightarrow CO_2 + H_2O \quad \text{heterotrophic respiration} \quad (1)$$~~

~~$$CH_4 + 2O_2 \leftrightarrow CO_2 + 2\,H_2O \quad \text{methane oxidation} \quad (2)$$~~

~~In case of intense methane oxidation, the 24-hour plots in Fig. 7 will approach a slope of -2 or an ecosystem quotient of -1/2. Other oxidative pathways of reduced substances like nitrification, consume oxygen and CO_2 which further steepens the slope of exO_2 vs. $exCO_2$. During the summer season this is indeed the case at Balanova station and less frequently at Busurca where conditions turned anoxic in May and July (Fig. 5). In both locations high methane concentrations were observed in previous surveys (Maier et al., 2022) and created conditions for intense oxygen consumption with only 50% CO_2 production.~~

~~Under conditions of intense photosynthesis, dissolved CO_2 will be depleted to low levels (Eq. 3), so that uptake of HCO_3^- will become a dominant pathway of photosynthesis, triggering calcite precipitation (Eq. 4) (Many et al., 2024):~~

~~$$CO_2 + H_2O \leftrightarrow \text{“}CH_2O\text{”} + O_2 \quad \text{photosynthesis} \quad (3)$$~~

~~$$2\,HCO_3^- + Ca^{2+} \leftrightarrow \text{“}CH_2O\text{”} + CaCO_3 + O_2 \quad \text{with calcite precipitation} \quad (4)$$~~

~~The slope of average daily $exCO_2$-exO_2 patterns turn steeper, as the importance of pathway 4 increases because O_2 is liberated without change in dissolved CO_2. There was considerable variability in the slopes from covariance and 24-h analysis (Table D1). Due to the larger amplitude of the day-night CO_2-O_2 cycles, the monthly slopes are better constrained in the summer months (April – Sept). Averaging the summer slopes of both the covariance and 24-hour analysis, yields 20 values; 8 of these calculated slopes were steeper than -2.0, 8 were in the range of -1.0 – -2 and 2 had an absolute value < 1. This synopsis provides strong evidence for methane oxidation, nitrification and other processes with high O_2-demand and limited CO_2-yield.~~

~~The lake system of Puiu-Rosu was an extreme case with summer slopes in the range of -6 to -10 and partial supersaturation with O_2 indicating uptake of HCO_3^- during calcite precipitation. (Fig. 7, Table D1). Additional evidence comes from the time series of conductivity measurements of the Balanova and Puiu-Rosu stations (Fig. 8). In June and July 2018, the conductivity sensor at the Puiu-Rosu lakes recorded a drop from 420 to less than 250 $\mu S\ cm^{-1}$ and pH reached day-time values of up to 9. The Balanova probe detected a weaker decline after a typical travel time of about 20 days and remained in a pH range below 8 indicating that low-conductivity lake water was mixed with water from the reed stands with higher dissolved CO_2 concentrations. Together these observations show that intense photosynthesis drove dissolved CO_2 to low levels in Lakes Puiu and Rosu. This favoured photosynthetic carbon uptake via HCO_3^- and triggered calcite precipitation and the drop in conductivity. The example confirms that freshwater carbonate buffering and calcite precipitation can play significant roles in carbon turnover in such shallow systems (Shangguan et al., 2025).~~

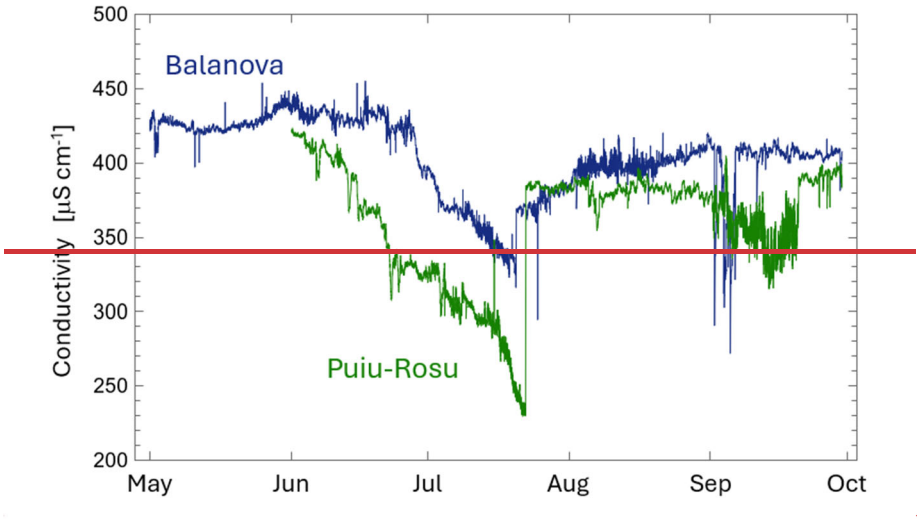

910

~~*Figure 8. Specific conductivity measured at 15' intervals at Balanova and Puiu-Rosu stations in 2018. The strong reduction in conductivity in the summer months indicates calcite precipitation.*~~

5. Conclusion

915 This study combined covariance analysis with averaging 24-h cycles of O_2-CO_2 pairs from sensor measurements at seven locations in the Danube Delta region. The dataset covered 105 monthly and about 3000 daily cycles. The results provide answers to the guiding questions outlined in the introduction:

- How does the intensity of river metabolism differ between the open waters of the delta compared to the upstream Danube River? Analysing the intensity of exO_2-$exCO_2$ dynamics revealed two orders of
920 magnitude difference in the amplitude of average diel cycles among stations and seasons with the lowest values during the cold season in the upstream stretch of Danube and the highest intensity in August at the the Balanova channel. ~~and a significantly more intense river metabolism within the delta compared to the three main river reaches of the Danube.~~ The monthly average of 24-h amplitudes and the stretch of exO_2-$exCO_2$ covariance ellipses consistently indicated a 4-8 times more intense aquatic ecosystem metabolism
925 within the delta compared to the main river branches.~~At monthly timescales, the stations within the delta showed 2-2.5 times higher daily amplitudes in exO_2-$exCO_2$ shifts. A daily analysis of potential drivers for river metabolism revealed a factor four stronger sensitivities towards cloud cover and water temperature within the delta compared to the river sections~~
- How significant is the contribution of lateral inflows from lake systems and reedbeds to the O_2 and CO_2
930 dynamics of the main river reaches crossing the delta? Wetland discharge could be identified by CO_2 rich water causing an offset with respect to the -1:1 exO_2:$exCO_2$ stoichiometry. Based on this indicator local wetland discharge was estimated as 13-25% of total discharge. These numbers exceed the total estimates of river diversion through the delta and should therefore be considered an upper limit. Balancing DIC increases along the final stretches of the main Danube branches revealed clear differences between low-
935 carbon inflow from lakes in Ukraine and high-carbon wetland discharge in the southern part of the Delta.

- What are the overall effects of river metabolism and wetland discharge on aquatic CO_2 emission rates in the Danube Delta? The $exCO_2$ records helped quantifying the magnitude of the wetland CO_2 pump in the Danube Delta. Overall, the downstream stations near the Black Sea exhibited $exCO_2$ values which were 1.7 to 2.1 times higher than at Tulcea. The estimated annual diffuse CO_2 emissions from water surface in the delta of 49 Gg C yr^{-1} were compatible with an earlier estimate based on more stations but less frequent sampling of 60 Gg C yr^{-1}. Estimates of the landscape-level CO_2 sink by the highly productive wetlands, however, are ~ 5 times higher.

In summary, the well-connected delta wetlands provide a boost in ecosystem metabolism which leaves clear signals of the wetland CO_2 pump in the lateral discharge reaching the main Danube branches. At the landscape scale, however, there is evidence from the literature that the highly productive wetland areas act as a net carbon sink.

~~Analysing the intensity of O_2-CO_2 dynamics revealed two orders of magnitude difference in the amplitude of average diel cycles among stations and seasons and a significantly more intense river metabolism within the delta compared to the three main river reaches of the Danube. At monthly timescales, the stations within the delta showed 2–2.5 times higher daily amplitudes in exO_2-$exCO_2$ shifts. A daily analysis of potential drivers for river metabolism revealed a factor four stronger sensitivities towards cloud cover and water temperature within the delta compared to the river sections.~~

~~The analysis of the shifting averages of excess O_2-CO_2 during an annual cycle allowed us to assess the importance and timing of lateral inflow of O_2-depleted and CO_2-oversaturated water from adjacent wetlands at monthly timescales. One of the channels drained anoxic wetland water with $exCO_2$ concentrations of almost 470 µM. At downstream Danube stations, strongest inflows from the wetlands were observed in connection to flood peaks in May – June and using an endmember model, these stations recorded mixtures of Danube water enriched by 5–20% wetland water. Attempts failed, however, to predict lateral inflows from upstream water levels due to unknown and variable flow paths and the complex hydrology of flood pulses and flood recession.~~

~~Slopes of O_2-CO_2 covariance ellipses and 24 hour cycles were in many cases significantly steeper than the slope of −1 predicted for a daily cycle of photosynthesis and respiration. Average monthly values for the warm season of April – September revealed ecosystem quotients $EQ < 0.5$ in 40% of the cases and another 40% were in the range of $0.5 < EQ < 1$. Together with the dominant oxygen undersaturation of the lower Danube and its delta system, this was a strong indication for the importance of additional processes with large O_2-demand and low CO_2 yield like methane oxidation and nitrification. In a monitored lake system, a calcite precipitation event was independently recorded by the conductivity sensor in June July and lead to very low ecosystem quotients EQ ~ 0.1 typical for HCO_3^- uptake during photosynthesis.~~

~~On a methodological level, the combination of covariance analysis with monthly averages of 24 h cycles provided a complementary perspective for a system, where lateral inflows obscure the in-stream metabolism at monthly timescales. The 24 h analysis provided additional insights into the timing and amplitude of the daily O_2-CO_2 cycles, whereas covariance analysis was a robust and rapid tool for exploring lateral inflows at monthly timescales and for quantifying metabolic drivers such as temperature and cloud cover at daily resolution.~~

6. Appendices

6.1 Appendix A – Monitoring stations

The monitoring stations were located upstream of the Delta at Tulcea and downstream ~~in~~ along the three branches of the Danube at St. George, Sulina and Chilia (Fig 1). During the ~~last~~ final year, the sensors were relocated to the Puiu-Rosu, Balanova, and Busurca ~~Channel~~ channels ~~and Puiu-Rosu~~ within the Delta. The t~~T~~ime coverage during the field campaign ~~was~~ ranged between 11 and ~~20~~ 21 months per station (Table A1). Spike removal at Sulina and Busurca reduced the number of observation days (Section 2.2.). Due to logistical ~~reasons~~ constraints the sensors were typically ~~mooring~~ moored ~~of the sensors was usually f~~from anchored boats (Fig. A1).

Table A1 Time series of O_2, ~~-~~CO_2 and DIC observations

Station	Latitude N	Longitude E	Start	End	Months *	Days **
Tulcea	45.218431°	28.751831°	11.04.2016	31.12.2017	18	534
Sulina	45.157878°	29.637892°	15.04.2016	31.12.2017	19	429
St. George	44.894163°	29.589989°	01.01.2016	31.12.2017	21	563
Chilia	45.252192°	29.660172°	01.01.2016	31.12.2016	12	308
Puiu-Rosu	45.050322°	29.496892°	12.02.2018	12.12.2018	11	302
Balanova	45.054968°	29.630634°	09.02.2018	13.12.2018	11	304
Busurca	45.158166°	29.610137°	10.02.2018	11.12.2018	11	248
Total					103	2688

*Months with >500 data, ** days with > 85 data

a)

b)

c)

d)

e)

f)

g)

h)

i)

990

Figure A1 *Characteristics of monitoring sites.*

~~a) a)~~ The Chilia site was located on the Romanian side of a small branch that defines the border with Ukraine. Despite ~~the~~ its location in a ~~side arm~~sidearm, the water ~~had~~ showed the same chemical signature as the main branch at the time of installation. ***b)*** *EXO2 probe at the Chilia ~~site~~ station during winter conditions.* ***c)*** *Clear ~~waters~~ water from the Busurca channel entering the Sulina reach of the Danube from the right. The Busurca monitoring station was located 25 m upstream of the ~~junction~~ confluence with the Sulina branch.* ***d)*** *Sulina ~~sensor~~station ~~-~~ located about 1 km downstream of Busurca junction and ~~. The Sulina probe was initially installed in the jetties but due to sporadic increases in specific conductivity, the probe was moved 3 km upstream in February 2016 to avoid disturbance by Black Sea water. It was~~ moored at an old, anchored ship.* ***e)*** *View from Tartaru channel ~~which was monitored at~~ close to Balanova station. The ~~towards the~~ Danube branch of St. George ~~Branch~~ in the background with ~~the~~ its turbid ~~Danube~~ water~~s~~ is flowing from left to right~~.~~ towards the Black Sea.* ***f)*** *For logistical reasons, the monitoring station at St. George branch was located about 500 m downstream of the confluence with the Tartaru ~~junction~~channel. The Black Sea is visible on the horizon.* ***g)*** *The Balanova multiprobe was deployed in the Central Channel connecting Sulina and St. George branches. The channel runs parallel to the gravel road linking two communities. The location is influenced by water originating from Lake Rosu. Balanova is a local name. ~~The Busurca probe was moored on a small, anchored houseboat.~~* ***h)*** *The Puiu-Rosu sensor recorded water quality at the outlet of Lake Puiu. The station was located on a small channel connecting Lake Puiu with Lake Rosu.* ***i)*** *The Busurca ~~Balanova~~ multiprobe was ~~placed~~ moored on a small, anchored houseboat. ~~in the Central Channel that connects Sulina and St. George main branches and runs in parallel to the gravel road connecting the two communities. The location is characterized by water from Lake Rosu that enters the Central Channel via the Andrei channel and splits north and south towards Sulina and St. George, respectively. At this location, water generally returns to the Danube after its journey through the intricate network of channels and lakes within the Delta.~~ Not shown: The Tulcea station~~, where sensors monitored~~ monitoring Danube water at the apex of the delta. The station was located 300 m downstream of the bifurcation ~~of~~ between the Tulcea and Chilia branches.*

6.2 Appendix B – Calculation of CO_2

The EXO2 sensors measured pH, temperature and specific conductivity at a frequency of 15 minutes. Using grab samples we correlated the continuous conductivity data with discrete lab-based alkalinity measurements (Raymond et al., 2013) and used the COSYS code (Van Heuven et al., 2011) to calculate dissolved CO_2 concentrations (Section 2.2).

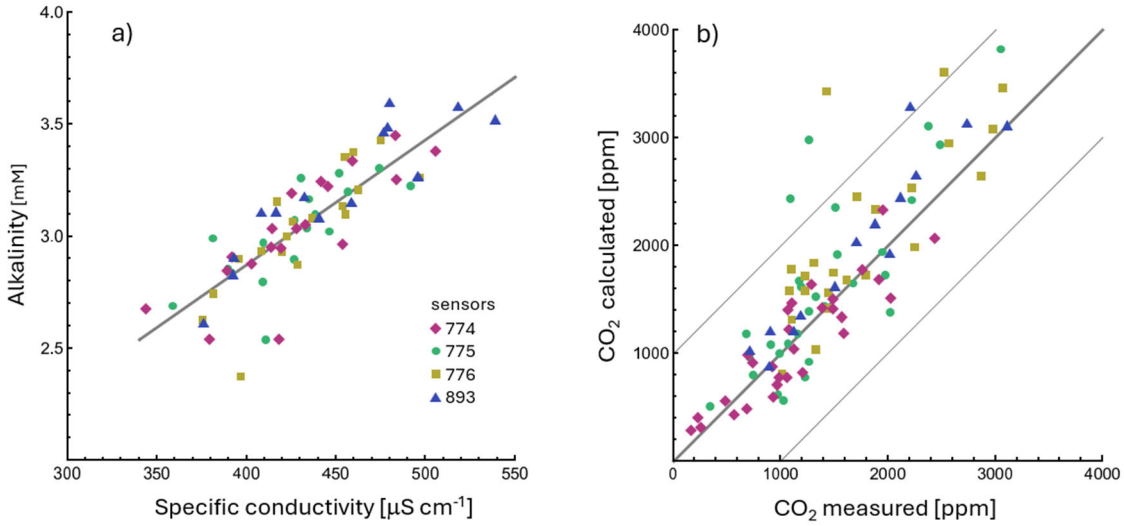

Figure B1 a) *Linear regression of alkalinity analyses ~~for~~ from water samples ~~and~~ versus specific conductivity. The specific conductivity recorded by the EXO2 sensors was correlated with alkalinity measurements obtained from titration analysis of water samples taken at the same time and location. Labels mark the four different EXO-2 probes. ~~deployed.~~ Alkalinity [mM] = 0.0057 × specific conductivity [µS cm^{-1}] + 0.60, with a correlation coefficient of R^2 = 0.70. ~~The specific conductivity recorded by the EXO2 sensors was correlated with alkalinity measurements obtained from titration analysis of water samples taken the same time and location. The coloured symbols mark the sensor codes, because the location of sensor packages changed during the three years of observations.~~*

b). *Measured CO_2 data based on the headspace technique compared to dissolved CO_2 calculated from EXO2 data ~~(specific conductivity, pH and temperature.~~ Alkalinity was estimated ~~from the~~by correlation ~~shown in(~~panel a) and pH plus temperature records were combined to calculate dissolved CO_2. ~~These~~ With few exceptions, the CO_2 estimates compared well with direct CO_2 measurements (R^2 = 0.82). ~~With few exceptions, the points lie well within~~Diagonal marks the 1:1 relationship with lines at ± 1000 ppm. Symbols represent the same sensors as in panel a).*

6.3 Appendix C DIC dynamics at Danube Delta stations~~Appendix C: Offset and slope~~

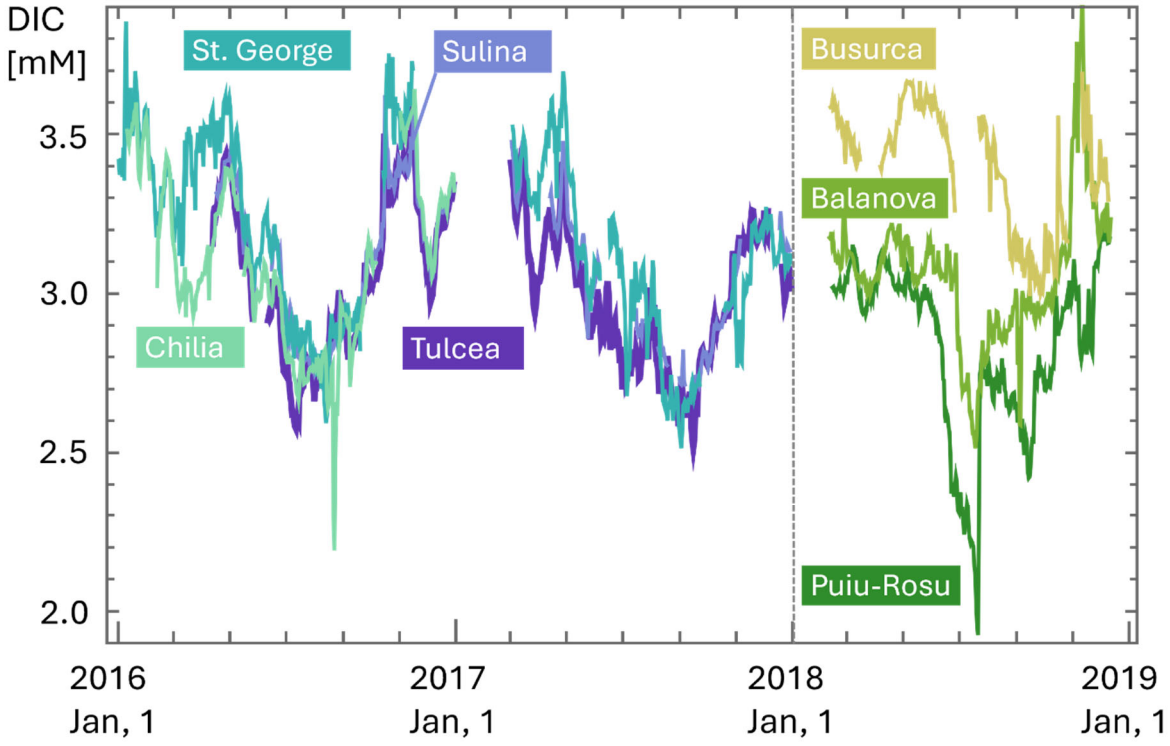

~~The offset can be defined with a positive or negative sign depending on the centroid position. Here we illustrate the definition and the construction of well-resolved offset timeseries (Fig. C1).~~

Figure C1 *Timeseries of DIC [µM] at the seven stations from January 2016 to December 2018. DIC based on measurements of conductivity, temperature, pH, and the calibration with titration alkalinity (Fig B1a).*

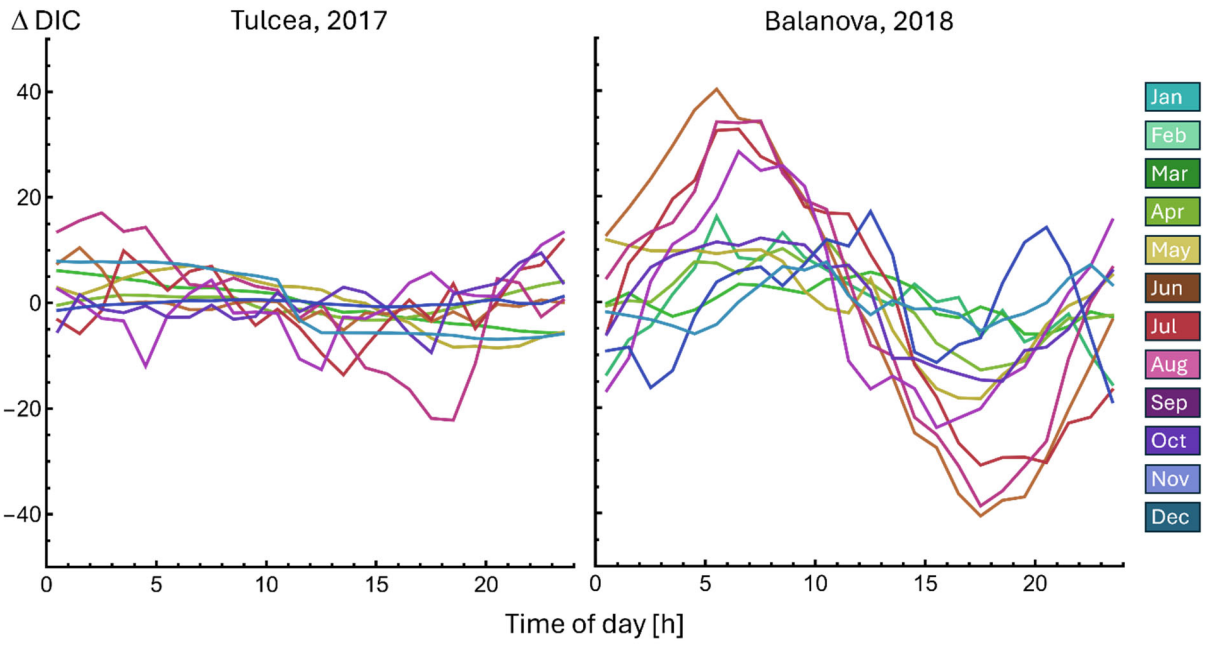

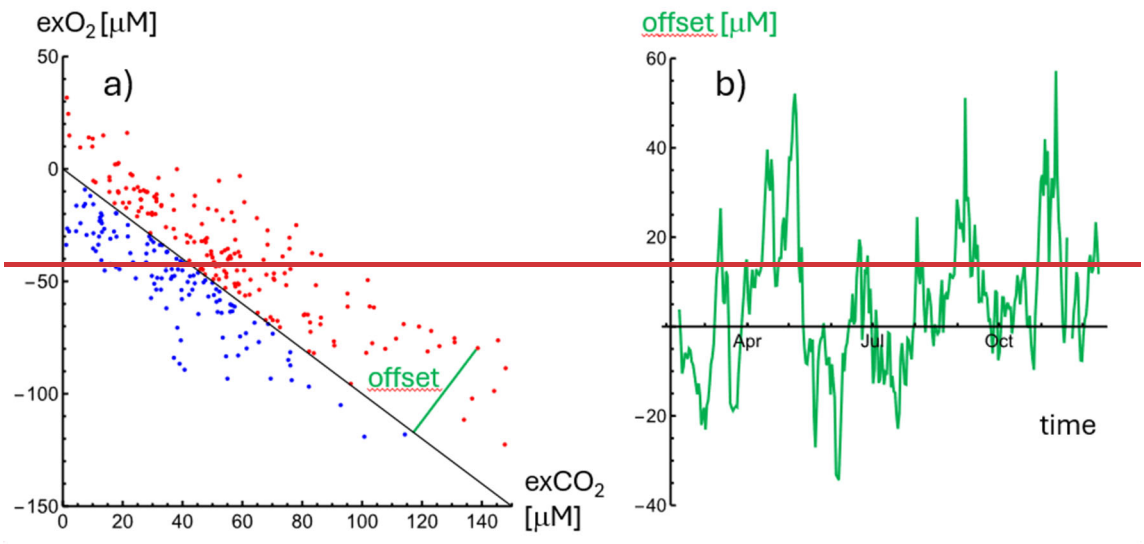

Figure C~~1~~2- *Example of 24-h monthly averages for DIC at Tulcea from March to December 2017 and at Balanova station from February to December 2018. The DIC cycles show stronger random variability compared to the exO_2 and $exCO_2$ cycles in Fig 3. Rapid changes in DIC at monthly timescales are likely and important source of this stochasticity (Fig C1).* ~~***a)*** *Daily centroids (average µM concentrations) of $exCO_2$ and exO_2 pairs at Balanova station in 2018. The closest distance between the dots and the line with slope -1 defines the offset. The green line shows an example. Blue dots are characterized by a negative offset and occur when high rates of photosynthesis and respiration reduce both O_2 and CO_2. We calculated the $\sum = exCO_2 + exO_2$ and defined a positive offset for $\sum > 0$, and negative offsets for $\sum < 0$.~~ ~~***b)*** *Time series of the resulting offset [µM] at Balanova station in 2018 shows phases where respiration dominates with a surplus in $exCO_2$ (positive offset) and periods in spring and summer when photosynthesis depleted the $exCO_2$ pool in comparison to exO_2. This time series with daily offsets is compatible with the trajectories of the monthly centroids (Fig. 5).~~

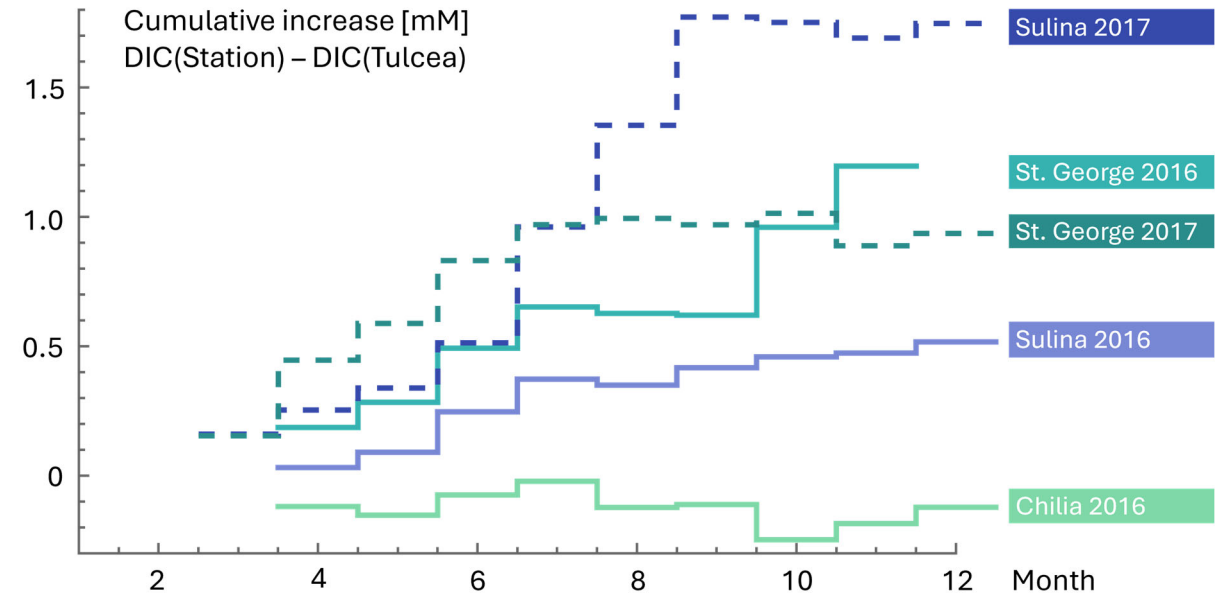

Figure C3 *Cumulative increase in DIC concentration during seasonal cycles calculated from the difference between the mean monthly DIC at a station and the upstream data at Tulcea.*

~~*The slopes of the stretch axes of the covariance ellipses (Fig 2) are defined by the Eigenvectors of the covariance matrix. By contrast, the slope of monthly averaged 24-hour cycles can be obtained from regression analysis. The slopes are related to the process stoichiometry of the river metabolism via the Ecosystem Quotient EQ = 1/s. Here we compare the two calculation methods.*~~

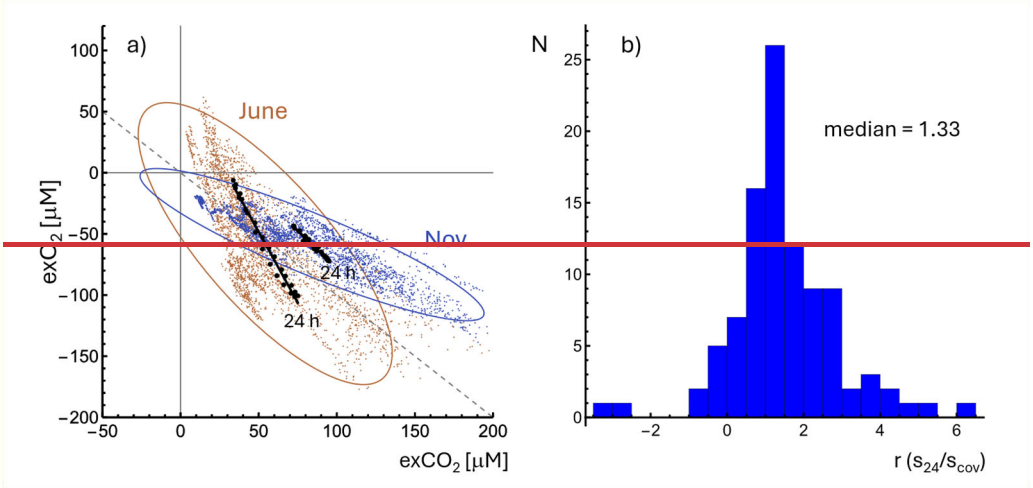

~~**Figure C2** *a) Examples of monthly covariance ellipses for June and November 2018 at Balanova. Black dots are the 24-hour monthly averages of daily fluctuations. The black regression lines show steeper slopes compared to the tilt of the covariance ellipses. b) Histogram of slope ratios* $r = s_{24}/s_{cov}$ **where** s_{24} **stands for the slope of the monthly averaged 24-hour cycle and** s_{cov} **refers to the tilt of the covariance ellipse calculated from the Eigenvectors of the covariance matrix. A total of 105 monthly records were analysed (Table D1). The median of r was 1.33 indicating that covariance analysis underestimates the slope of the day-night cycles. In the Danube Delta lateral inflow of CO_2-rich water shifts the daily O_2-CO_2 cycles on the horizontal axis which decreases the observed average monthly slope. To avoid this artifact, slopes and corresponding ecosystem quotients EQ should preferably be calculated from averaged 24-hour cycles.**~~

6.4 Appendix D Overview of 24-h cycles

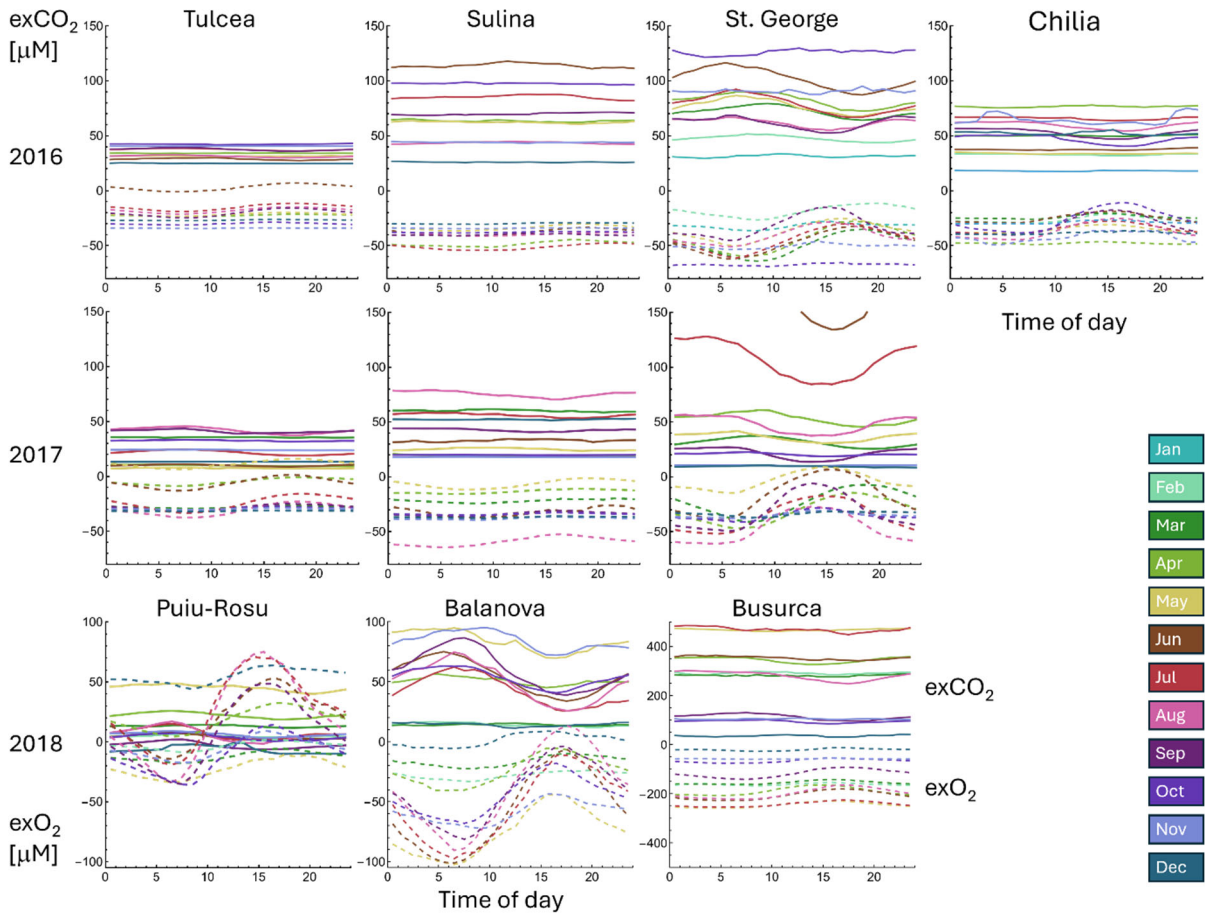

1090

~~Appendix D: Results from 24-h averaging and covariance analysis~~

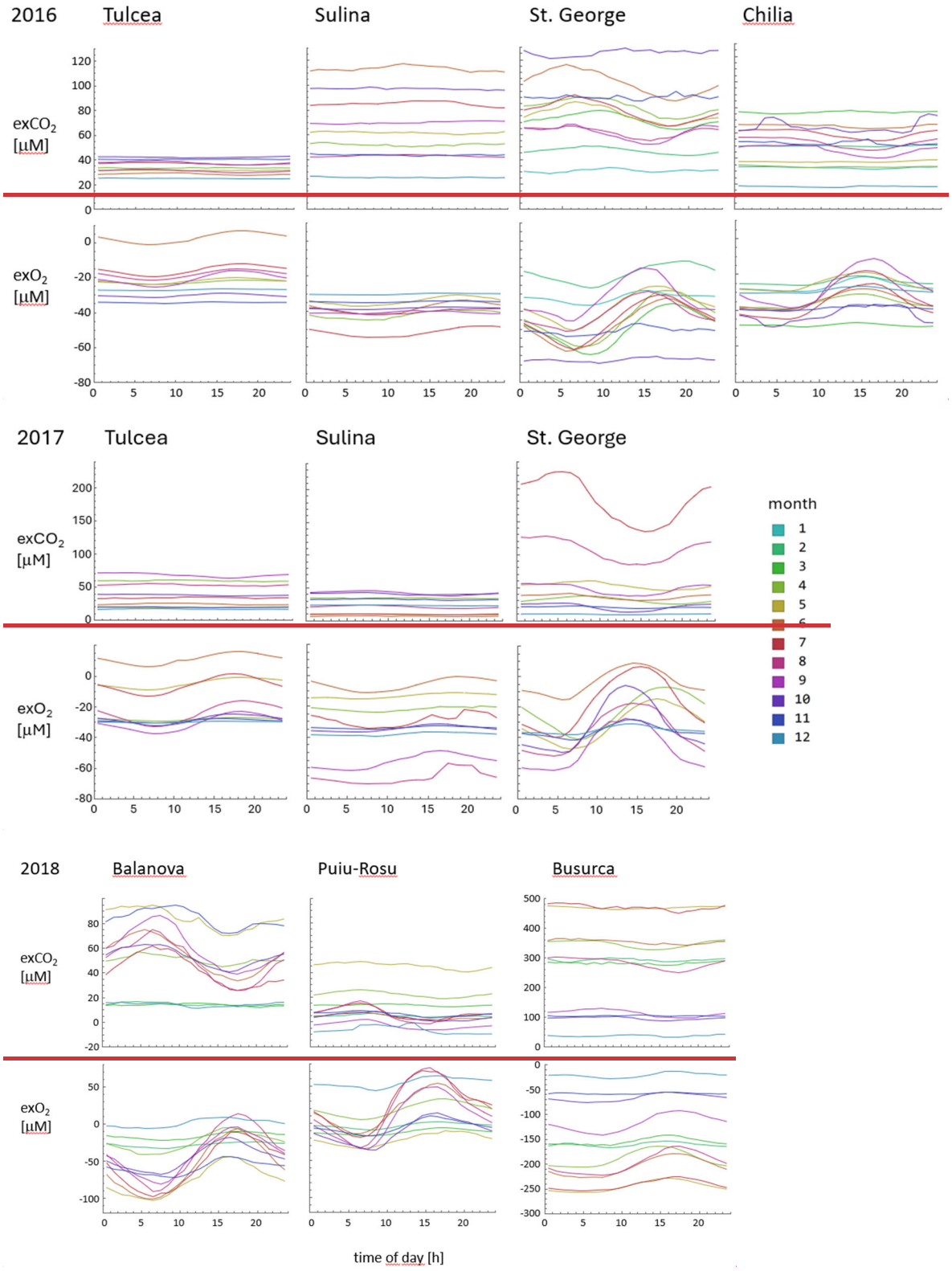

1095

Figure ~~D1~~D1. *Monthly averaged time-of-day plots ~~at 15-minute resolution~~ showing ~~excess~~ exCO_2 (solid lines) and exO_2 (dashed) ~~for the years~~during 2016 and 2017 at the Danube stations ~~of Tulcea, Sulina, St. George, and Chilia and for the three stations within the~~during ~~Delta in~~ 2018 at the Delta stations~~. Note that the months are~~*

~~color coded and y-axes in 2016 and 2017 differ~~. ~~In comparison to Balanova and Puiu-Rosu, data from the Busurca Channel are plotted with an extended y-axis.~~Extended y-axis for Busurca.

~~**Table D1** Results of monthly covariance analysis. Centroid position c-$exCO_2$ and c-exO_2, stretch, width and offset [µM], slope [ ]. Maximum number of observations (ndata) for 31 days is 2976., slope 24 refers to the slope calculated from 24-h averaging (Fig 7, Fig S4f)), nd = no data.~~

Station	parameter	Jan	Feb	Mar	Apr	May	Jun	Jul	Aug	Sept	Oct	Nov	Dec
Tulcea	ndata	1793	nd	nd	1879	2468	1967	2971	2971	2875	2970	2874	2770
2016	c-$exCO_2$	35.9	nd	nd	33.8	31.3	28.5	37.2	31.2	37.4	42.1	40.4	24.7
	c-exO_2	-26.8	nd	nd	-22.7	-21.8	2.8	-15.5	-18.2	-20.6	-30.3	-34.3	-26.9
	stretch	11.8	nd	nd	19.7	42.2	54.5	46.3	40.1	30.9	38.8	13.0	16.4
	width	5.4	nd	nd	4.5	11.3	16.7	20.6	10.3	10.6	6.6	4.9	4.6
	offset	6.4	nd	nd	7.8	6.7	22.2	15.4	9.2	11.9	8.3	4.3	1.5
	slope	0.6	nd	nd	-1.3	-1.4	-1.7	-1.9	-3.6	-1.8	-1.7	-0.7	-0.6
	slope 24	nd	nd	nd	-3.6	-3.7	-3.4	-3.5	-2.6	-2.7	-1.2	+0.3	-1.3
Tulcea	ndata	nd	nd	2976	2873	2969	2873	2969	2969	2872	2619	2875	1822
2017	c-$exCO_2$	nd	nd	35.6	9.9	7.5	10.1	21.6	41.9	41.1	32.7	23.9	13.3
	c-exO_2	nd	nd	-27.9	-4.8	11.3	-5.9	-24.2	-30.6	-28.2	-29.2	-29.7	-31.5
	stretch	nd	nd	29.7	51.2	78.0	61.1	64.4	54.3	35.6	20.1	14.0	7.7
	width	nd	nd	7.5	17.7	6.3	12.1	15.1	11.0	11.2	9.2	6.5	5.3
	offset	nd	nd	5.4	3.7	13.3	2.9	1.8	8.0	9.1	2.4	4.1	12.9
	slope	nd	nd	-4.3	-1.9	-3.1	-6.0	-1.9	-1.5	-0.9	-1.9	0.4	-1.5
	slope 24	nd	nd	-2.4	-4.5	-8.2	-6.5	-3.1	-1.8	-1.3	-1.7	-1.3	-0.6
St George	ndata	2971	2779	2971	2875	2971	2876	2972	2971	1872	1774	1486	nd
2016	c-$exCO_2$	31.0	47.2	71.8	81.9	76.3	101.6	78.7	61.9	61.7	125.8	90.2	nd
	c-exO_2	-32.3	-18.7	-49.5	-44.3	-37.3	-47.2	-44.8	-41.1	-32.6	-67.3	-50.7	nd
	stretch	28.0	42.6	50.4	63.7	53.2	59.8	45.7	38.9	37.8	73.5	48.9	nd
	width	18.1	9.9	20.3	20.5	18.0	14.7	17.0	17.6	12.4	13.9	22.8	nd
	offset	0.9	20.2	15.8	26.6	27.6	38.5	23.9	14.7	20.5	41.3	27.9	nd
	slope	-1.3	-1.6	-1.0	-1.0	-0.9	-0.8	-0.9	-1.1	-1.4	-0.4	-0.4	nd
	slope 24	-0.7	-2.0	-1.9	-1.8	-1.2	-1.0	-1.2	-1.9	-1.8	+0.1	-0.5	nd
St George	ndata	nd	nd	2818	2873	2967	2149	2970	2963	2184	1299	2874	2770
2017	c-$exCO_2$	nd	nd	31.3	53.2	36.1	180.7	106.8	48.0	21.5	20.6	10.4	9.3
	c-exO_2	nd	nd	-22.9	-31.2	-3.7	-17.0	-36.2	-46.9	-32.2	-35.5	-35.0	-33.5
	stretch	nd	nd	44.9	68.8	62.1	225.0	151.3	76.0	50.2	16.4	13.1	16.8
	width	nd	nd	16.1	27.8	16.6	38.4	55.8	27.9	15.1	12.9	7.6	12.2
	offset	nd	nd	6.0	15.5	22.9	115.7	49.9	0.7	7.6	10.5	17.4	17.1
	slope	nd	nd	-2.3	-0.9	-1.7	-0.2	0.0	-0.7	-2.2	-3.5	-6.4	-0.6
	slope 24	nd	nd	-2.9	-2.1	-2.1	-0.5	-0.8	-1.8	-3.1	-3.2	-5.6	-3.1
Sulina	ndata	nd	nd	nd	792	2692	1593	2969	2967	2487	2969	2872	2966
2016	c-$exCO_2$	nd	nd	nd	52.3	62.0	113.7	85.2	43.3	69.9	97.3	43.8	25.8
	c-exO_2	nd	nd	nd	-41.5	-34.0	-37.9	-51.7	-39.8	-40.3	-38.0	-34.4	-30.1
	stretch	nd	nd	nd	18.9	50.3	58.4	52.8	24.7	44.4	59.9	21.2	18.4
	width	nd	nd	nd	7.8	13.6	16.8	21.1	14.3	12.2	16.3	8.1	5.1
	offset	nd	nd	nd	7.7	19.8	53.6	23.7	2.5	20.9	41.9	6.7	3.0
	slope	nd	nd	nd	-1.3	-0.5	-0.5	0.0	-4.9	-0.6	-0.3	-0.3	-0.9
	slope 24	nd	nd	nd	-0.2	-2.2	-0.6	-0.7	-1.3	+0.1	-0.4	-0.3	-0.6

Table D2 – continued

Station	parameter	Jan	Feb	Mar	Apr	May	Jun	Jul	Aug	Sept	Oct	Nov	Dec
Sulina	ndata	nd	nd	1380	1761	2971	1046	1424	1366	1985	2758	510	1382
2017	c-exCO$_2$	nd	nd	60.3	19.5	25.1	34.1	53.8	68.8	38.5	19.9	18.1	52.3
	c-exO$_2$	nd	nd	-21.9	-13.3	-6.3	-29.3	-66.1	-55.8	-34.5	-33.8	-38.0	-36.7
	stretch	nd	nd	24.6	33.7	71.6	49.1	100.6	40.1	31.1	12.7	9.3	15.7
	width	nd	nd	14.5	19.5	13.3	19.7	40.2	17.7	11.2	6.7	1.2	4.8
	offset	nd	nd	27.2	4.4	13.3	3.4	8.6	9.2	2.8	9.8	14.1	11.0
	slope	nd	nd	-2.1	-1.4	-1.6	-2.4	-3.0	-1.2	-0.8	11.0	-3.3	-0.4
	slope-24	nd	nd	-2.4	-4.5	-8.2	-6.5	-3.1	-1.8	-1.2	-1.7	-1.3	-0.6
Chilia	ndata	2616	2247	2970	2874	2486	2873	2969	2964	2716	1620	2611	2894
2016	c-exCO$_2$	32.7	49.8	76.3	33.7	37.4	65.5	59.2	52.3	46.4	64.5	52.1	17.9
	c-exO$_2$	-26.6	-24.0	-48.1	-35.7	-25.2	-34.7	-36.5	-31.4	-26.2	-42.3	-38.8	-29.0
	stretch	17.6	21.3	29.5	29.2	48.0	39.4	37.7	42.8	79.2	65.1	29.7	24.3
	width	9.7	7.3	23.7	11.9	11.1	13.9	17.3	17.6	12.5	12.6	10.9	6.5
	offset	4.4	18.2	19.9	1.4	8.6	21.8	16.1	14.8	14.3	15.7	9.4	7.9
	slope	4.8	-0.5	-1.0	-0.9	-0.8	-0.8	-0.8	-1.8	-1.6	-0.6	-0.4	-0.8
	slope-24	-3.8	-2.2	+0.4	-3.0	-2.3	-3.2	-2.3	-2.3	-2.5	-0.7	-0.1	+0.5
Balanova	ndata	nd	1859	2976	2874	2969	2875	2971	2971	2875	2971	2776	1211
2018	c-exCO$_2$	nd	14.2	14.0	50.5	83.7	54.2	42.5	49.4	60.1	53.3	84.2	14.2
	c-exO$_2$	nd	-28.1	-16.4	-24.3	-75.4	-58.0	-54.9	-38.5	-41.5	-45.4	-58.8	1.2
	stretch	nd	27.6	46.4	74.5	113.4	133.9	124.5	133.1	119.1	59.3	124.2	53.7
	width	nd	15.7	21.2	29.7	54.4	44.3	28.8	36.2	38.7	23.0	23.7	13.7
	offset	nd	9.8	1.7	18.6	5.9	2.7	8.8	7.7	13.1	5.6	18.0	10.9
	slope	nd	-1.7	-31.4	-0.9	-0.6	-1.6	-1.6	-1.3	-1.0	-1.7	-0.5	-1.9
	slope-24	nd	-1.8	-2.9	-3.5	-2.3	-2.3	-2.4	-2.1	-1.6	-2.2	-1.2	-2.9
Busurca	ndata	nd	1767	1513	2455	2860	2452	1011	2417	2868	2972	2874	1020
2018	c-exCO$_2$	nd	291	282	346	468	354	469	280	113	94.7	104	36.3
	c-exO$_2$	nd	-161	-154	-188	-245	-206	-241	-197	-117	-65.8	-57.7	-20.3
	stretch	nd	111.8	65.4	167.9	90.8	165.0	68.5	265.9	137.3	93.2	146.3	53.2
	width	nd	19.2	32.9	26.5	35.8	45.2	45.6	56.0	40.9	46.9	41.2	27.8
	offset	nd	92.3	90.6	111.4	157.5	104.6	161.3	58.8	2.4	20.4	33.0	11.3
	slope	nd	-0.3	-0.2	-0.6	-0.2	-0.3	0.1	-0.4	-1.2	-0.9	-0.4	-2.6
	slope-24	nd	-0.7	-1.2	-1.4	-0.6	-2.2	-0.8	-1.1	-1.5	-1.4	-0.3	-0.6
PuiuRosu	ndata	nd	1575	2976	2875	2969	2875	2969	2971	2875	2971	2874	1110
2018	c-exCO$_2$	nd	5.0	13.2	22.2	45.1	3.9	7.2	6.5	-2.8	4.0	6.2	-6.3
	c-exO$_2$	nd	-3.0	-12.1	18.4	-21.9	19.3	26.4	19.6	6.7	-10.8	-5.2	54.6
	stretch	nd	20.2	63.0	35.9	75.1	135.4	133.7	127.6	98.4	78.3	69.0	64.9
	width	nd	17.8	31.5	34.6	39.8	17.9	21.2	26.7	8.9	15.8	17.8	31.1
	offset	nd	1.4	0.8	28.7	16.4	16.4	23.7	18.5	2.7	4.8	0.7	34.1
	slope	nd	24.2	-1.2	-0.4	0.1	-7.8	-5.6	-5.3	-10.0	-3.9	-1.8	-5.4
	slope-24	nd	-3.89	-4.2	-4.2	-2.6	-9.7	-6.9	-6.1	-10.0	-6.3	-4.5	-1.2

7. Code availability

The Mathematica code is available as a notebook file at GitHub https://github.com/bernhardwehrli/CO2-O2-stat

8. Data availability

Timeseries data and the calculated daily covariance parameters for all stations are available at the ETH research collection via https://doi.org/10.3929/ethz-c-000786936

9. Author contributions

Field campaigns and statistical analyses were designed with input from all authors, BW provided project supervision, CT led the monitoring campaigns and data collection, MSM contributed to field work and was responsible for laboratory analyses, quality control and ~~post-processing and quality control of~~calculating ~~field data and calculated the~~ $exCO_2$, ~~and~~ exO_2 and DIC timeseries. BW led the coding, drafting and writing of the paper with continuous input from MSM and CT.

10. Competing interests

The authors declare that they have no conflict of interest.

11. Acknowledgements

~~The authors~~We thank Christian Dinkel, Patrick Kathriner and Tim Kalvelage for their support during fieldwork and lab analyses. The authors are grateful for constructive reviews and comments by Ji-Hyung Park, Jacob Diamond and an anonymous reviewer which helped to significantly improve an earlier version of the manuscript.~~

12. Financial support

This study was supported by the Swiss State Secretariat for Education, Research and Innovation (SERI; grant no. 15.0068). The research consortium received funding from the European Union's Horizon 2020 research and innovation programme under the Marie- Skłodowska-Curie-Actions (grant no. 643052; C-CASCADES project). The Swiss National Science Foundation (SNF) and Eawag provided funding for the EXO2 probes (R'EQUIP 157750).

13. References

Abril, G. and Borges, A. V.: Ideas and perspectives: Carbon leaks from flooded land: do we need to replumb the inland water active pipe?, Biogeosciences, 16, 769-784, 10.5194/bg-16-769-2019, 2019.

Aho, K. S., Hosen, J. D., Logozzo, L. A., McGillis, W. R., and Raymond, P. A.: Highest rates of gross primary productivity maintained despite CO_2 depletion in a temperate river network, Limnology and Oceanography Letters, 6, 200-206, 10.1002/lol2.10195, 2021.

Battin, T. J., Lauerwald, R., Bernhardt, E. S., Bertuzzo, E., Gener, L. G., Hall, R. O., Jr., Hotchkiss, E. R., Maavara, T., Pavelsky, T. M., Ran, L., Raymond, P., Rosentreter, J. A., and Regnier, P.: River ecosystem metabolism and carbon biogeochemistry in a changing world, Nature, 613, 449-459, 10.1038/s41586-022-05500-8, 2023.

Bernhardt, E. S., Heffernan, J. B., Grimm, N. B., Stanley, E. H., Harvey, J. W., Arroita, M., Appling, A. P., Cohen, M. J., McDowell, W. H., Hall, R. O., Read, J. S., Roberts, B. J., Stets, E. G., and Yackulic, C. B.: The metabolic regimes of flowing waters, Limnology and Oceanography, 63, 10.1002/lno.10726, 2017.

Bertassello, L. E., Basu, N. B., Maes, J., Grizzetti, B., La Notte, A., and Feyen, L.: The important role of wetland conservation and restoration in nitrogen removal across European river basins, Nature Water, 3, 10.1038/s44221-025-00465-0, 2025.

Bondar, C.: Referitor la alimentarea si tranzitul apelor Dunarii prin interiorul deltei, Analele ICPDD, III/2, 259-261, 1994.

Borges, A. V., Darchambeau, F., Lambert, T., Morana, C., Allen, G. H., Tambwe, E., Sembaito, A. T., Mambo, T., Wabakhangazi, J. N., Descy, J. P., Teodoru, C. R., and Bouillon, S.: Variations in dissolved greenhouse gases (CO_2, CH_4, N_2O) in the Congo River network overwhelmingly driven by fluvial-wetland connectivity, Biogeosciences, 16, 3801-3834, 10.5194/bg-16-3801-2019, 2019.

Cai, W. J. and Wang, Y.: The chemistry, fluxes, and sources of carbon dioxide in the estuarine waters of the Satilla and Altamaha Rivers, Georgia, Limnology and Oceanography, 43, 657-668, 1998.

Canning, A., Wehrli, B., and Körtzinger, A.: Methane in the Danube Delta: the importance of spatial patterns and diel cycles for atmospheric emission estimates, Biogeosciences, 18, 3961-3979, 10.5194/bg-18-3961-2021, 2021.

Cole, J. J., Prairie, Y. T., Caraco, N. F., McDowell, W. H., Tranvik, L. J., Striegl, R. G., Duarte, C. M., Kortelainen, P., Downing, J. A., Middelburg, J. J., and Melack, J.: Plumbing the Global Carbon Cycle: Integrating Inland Waters into the Terrestrial Carbon Budget, Ecosystems, 10, 172-185, 10.1007/s10021-006-9013-8, 2007.

Coops, H., Buijse, L. L., Buijse, A. D., Constantinescu, A., Covaliov, S., Hanganu, J., Ibelings, B. W., Menting, G., Navodaru, I., Oosterberg, W., Staras, M., and Török, L.: Trophic gradients in a large-river Delta: ecological structure determined by connectivity gradients in the Danube Delta (Romania), River Research and Applications, 24, 698-709, 10.1002/rra.1136, 2008.

Csagoly, P., Magnin, G., and Hulea, O.: Lower Danube Green Corridor, in: The Wetland Book., edited by: Finlayson, C. M., Milton, G., Prentice, R., and Davidson, N., Springer, Dodrecht, https://doi.org/10.1007/978-94-007-4001-3_251, 2018.

Dalmagro, H. J., Lathuilliere, M. J., Hawthorne, I., Morais, D. D., Pinto, O. B., Couto, E. G., and Johnson, M. S.: Carbon biogeochemistry of a flooded Pantanal forest over three annual flood cycles, Biogeochemistry, 139, 1-18, 10.1007/s10533-018-0450-1, 2018.

Degens, E., Kempe, S., and Ittekkot, V.: Monitoring carbon in world rivers, Environment: Science and Policy for Sustainable Development, 26, 29-33, 10.1080/00139157.1984.9932533, 1984.

Deirmendjian, L. and Abril, G.: Carbon dioxide degassing at the groundwater-stream-atmosphere interface: isotopic equilibration and hydrological mass balance in a sandy watershed, Journal of Hydrology, 558, 129-143, 10.1016/j.jhydrol.2018.01.003, 2018.

DelVecchia, A. G., Rhea, S., Aho, K. S., Stanley, E. H., Hotchkiss, E. R., Carter, A., and Bernhardt, E. S.: Variability and drivers of CO_2, CH_4, and N_2O concentrations in streams across the United States, Limnology and Oceanography, 68, 394-408, 10.1002/lno.12281, 2023.

Diamond, J. S. and Bertuzzo, E.: A Coupled O_2-CO_2 Model for Joint Estimation of Stream Metabolism, O-C Stoichiometry, and Inorganic Carbon Fluxes, Journal of Geophysical Research-Biogeosciences, 130, 10.1029/2024jg008401, 2025.

Diamond, J. S., Truong, A. N., Abril, G., Bertuzzo, E., Chanudet, V., Lamouroux, R., and Moatar, F.: Inorganic carbon dynamics and their relation to autotrophic community regime shift over three decades in a large, alkaline river, Limnology and Oceanography, 70, 1122-1136, 10.1002/lno.70016, 2025.

Dodds, W. K., Veach, A. M., Ruffing, C. M., Larson, D. M., Fischer, J. L., and Costigan, K. H.: Abiotic controls and temporal variability of river metabolism: multiyear analyses of Mississippi and Chattahoochee River data, Freshwater Science, 32, 1073-1087, 10.1899/13-018.1, 2013.

Dybdahl, A. K., Holmboe, C. M. H., Baattrup-Pedersen, A., Riis, T., and Pastor, A.: Temperature dependence of biofilm metabolism in a lowland stream, Freshwater Science, 43, 277-287, 10.1086/731873, 2024.

Gatescu, P., Driga, B., and Angel, C.: Caracteristici morfohidrografice ale Deltei Dunarii, Hidrobiologia, Acad. Rom. Bucuresti1983.

Gomez-Baggethun, E., Tudor, M., Doroftei, M., Covaliov, S., Nastase, A., Onara, D. F., Mierla, M., Marinov, M., Dorosencu, A. C., Lupu, G., Teodorof, L., Tudor, I. M., Kohler, B., Museth, J., Aronsen, E., Johnsen, S. I., Ibram, O., Marin, E., Craciun, A., and Cioaca, E.: Changes in ecosystem services from wetland loss and restoration: An ecosystem assessment of the Danube Delta (1960-2010), Ecosyst. Serv., 39, 17, 10.1016/j.ecoser.2019.100965, 2019.

Gomez-Gener, L., Rocher-Ros, G., Battin, T., Cohen, M. J., Dalmagro, H. J., Dinsmore, K. J., Drake, T. W., Duvert, C., Enrich-Prast, A., Horgby, A., Johnson, M. S., Kirk, L., Machado-Silva, F., Marzolf, N. S., McDowell, M. J., McDowell, W. H., Miettinen, H., Ojala, A. K., Peter, H., Pumpanen, J., Ran, L. S., Riveros-Iregui, D. A., Santos, I. R., Six, J., Stanley, E. H., Wallin, M. B., White, S. A., and Sponseller, R. A.: Global carbon dioxide efflux from rivers enhanced by high nocturnal emissions, Nature Geoscience, 14, 289-+, 10.1038/s41561-021-00722-3, 2021.

Haque, M. M., Begum, M. S., Nayna, O. K., Tareq, S. M., and Park, J.-H.: Seasonal shifts in diurnal variations of CO_2 and O_2 in the lower Ganges River, Limnology and Oceanography Letters, 7, 191-201, 10.1002/lol2.10246, 2022.

Hastie, A., Lauerwald, R., Ciais, P., and Regnier, P.: Aquatic carbon fluxes dampen the overall variation of net ecosystem productivity in the Amazon basin: An analysis of the interannual variability in the boundless carbon cycle, Glob Chang Biol, 25, 2094-2111, 10.1111/gcb.14620, 2019.

Hemes, K. S., Chamberlain, S. D., Eichelmann, E., Knox, S. H., and Baldocchi, D. D.: A Biogeochemical Compromise: The High Methane Cost of Sequestering Carbon in Restored Wetlands, Geophysical Research Letters, 45, 6081-6091, 10.1029/2018gl077747, 2018.

Hotchkiss, E. R., Hall Jr, R. O., Sponseller, R. A., Butman, D., Klaminder, J., Laudon, H., Rosvall, M., and Karlsson, J.: Sources of and processes controlling CO_2 emissions change with the size of streams and rivers, Nature Geoscience, 8, 696-699, 10.1038/ngeo2507, 2015.

Huertas, I. E., Flecha, S., Figuerola, J., Costas, E., and Morris, E. P.: Effect of hydroperiod on CO_2 fluxes at the air-water interface in the Mediterranean coastal wetlands of Donana, Journal of Geophysical Research-Biogeosciences, 122, 1615-1631, 10.1002/2017JG003793, 2017.

Jankowski, K., Schindler, D. E., and Lisi, P. J.: Temperature sensitivity of community respiration rates in streams is associated with watershed geomorphic features, Ecology, 95, 2707-2714, 10.1890/14-0608.1, 2014.

Kathilankal, J. C., O'Halloran, T. L., Schmidt, A., Hanson, C. V., and Law, B. E.: Development of a semi-parametric PAR (Photosynthetically Active Radiation) partitioning model for the United States, version 1.0, Geoscientific Model Development, 7, 2477-2484, 10.5194/gmd-7-2477-2014, 2014.

Li, J. J., Yuan, J. J., Ciais, P., Kang, H. J., Freeman, C., Huang, Y. Y., Dong, Y. H., Liu, D. Y., Li, Y., and Ding, W. X.: Two decades of improved wetland carbon sequestration in northern mid-to-high latitudes are offset by tropical and southern declines, Nature Ecology & Evolution, 9, 10.1038/s41559-025-02809-1, 2025.

Lu, W. Z., Xiao, J. F., Liu, F., Zhang, Y., Liu, C. A., and Lin, G. H.: Contrasting ecosystem CO2 fluxes of inland and coastal wetlands: a meta-analysis of eddy covariance data, Global Change Biology, 23, 1180-1198, 10.1111/gcb.13424, 2017.

Maier, M.-S., Teodoru, C. R., and Wehrli, B.: Spatio-temporal variations in lateral and atmospheric carbon fluxes from the Danube Delta, Biogeosciences, 18, 1417-1437, 10.5194/bg-18-1417-2021, 2021.

Maier, M.-S., Canning, A. R., Brennwald, M. S., Teodoru, C. R., and Wehrli, B.: Spatial Mapping of Dissolved Gases in the Danube Delta Reveals Intense Plant-Mediated Gas Transfer, Frontiers in Environmental Science, 10, 10.3389/fenvs.2022.838126, 2022.

Many, G., Escoffier, N., Perolo, P., Barenbold, F., Bouffard, D., and Perga, M. E.: Calcite precipitation: The forgotten piece of lakes' carbon cycle, Science Advances, 10, eado5924, 10.1126/sciadv.ado5924, 2024.

Marzolf, N. S., Small, G. E., Oviedo-Vargas, D., Ganong, C. N., Duff, J. H., Ramirez, A., Pringle, C. M., Genereux, D. P., and Ardon, M.: Partitioning inorganic carbon fluxes from paired O_2-CO_2 gas measurements in a Neotropical headwater stream, Costa Rica, Biogeochemistry, 160, 259-273, 10.1007/s10533-022-00954-4, 2022.

Mayr, M. J., Zimmermann, M., Dey, J., Brand, A., Wehrli, B., and Burgmann, H.: Growth and rapid succession of methanotrophs effectively limit methane release during lake overturn, Communications Biology, 3, 108, 10.1038/s42003-020-0838-z, 2020.

Mulholland, P. J., Fellows, C. S., Tank, J. L., Grimm, N. B., Webster, J. R., Hamilton, S. K., Martí, E., Ashkenas, L., Bowden, W. B., Dodds, W. K., McDowell, W. H., Paul, M. J., and Peterson, B. J.: Inter-biome comparison of factors controlling stream metabolism, Freshwater Biology, 46, 1503-1517, 10.1046/j.1365-2427.2001.00773.x, 2001.

Nguyen, A. T., Abril, G., Diamond, J. S., Lamouroux, R., Martinet, C., and Moatar, F.: Multidecadal trends in CO2 evasion and aquatic metabolism in a large temperate river, Biogeosciences, 22, 4923-4951, 10.5194/bg-22-4923-2025, 2025.

Oosterberg, W., Staras, M., Bodgdan, L., Buijse, A. D., Constantinescu, A., Coops, H., Hanganu, J., Ibelings, B. W., Menting, G. A. M., and Navodaru, I.: Ecological gradients in the Danube Delta lakes: present state and man-induced changes, RIZA, Rijkswaterstaat, NL, 2000.

Oprea, A., SÎRbu, C., Doroftei, M., and Covaliov, S.: New Contributions to Vegetation Knowledge of the Danube Delta, Romania (I), Journal of Plant Development, 31, 159-181, 10.47743/jpd.2024.31.1.958, 2024.

Oswald, K., Milucka, J., Brand, A., Hach, P., Littmann, S., Wehrli, B., Kuypers, M. M. M., and Schubert, C. J.: Aerobic gammaproteobacterial methanotrophs mitigate methane emissions from oxic and anoxic lake waters, Limnology and Oceanography, 61, 10.1002/lno.10312, 2016.

Perkins, D. M., Yvon-Durocher, G., Demars, B. O. L., Reiss, J., Pichler, D. E., Friberg, N., Trimmer, M., and Woodward, G.: Consistent temperature dependence of respiration across ecosystems contrasting in thermal history, Global Change Biology, 18, 1300-1311, 10.1111/j.1365-2486.2011.02597.x, 2012.

Rabaey, J. S., Holgerson, M. A., Richardson, D. C., Andersen, M. R., Bansal, S., Bortolotti, L. E., Cotner, J. B., Hornbach, D. J., Martinsen, K. T., Moody, E. K., and Schloegel, O. F.: Freshwater Biogeochemical Hotspots: High Primary Production and Ecosystem Respiration in Shallow Waterbodies, Geophysical Research Letters, 51, 10.1029/2023gl106689, 2024.

Raymond, P. A., Hartmann, J., Lauerwald, R., Sobek, S., McDonald, C., Hoover, M., Butman, D., Striegl, R., Mayorga, E., Humborg, C., Kortelainen, P., Durr, H., Meybeck, M., Ciais, P., and Guth, P.: Global carbon dioxide emissions from inland waters, Nature, 503, 355-359, 10.1038/nature12760, 2013.

Reiman, J. H. and Xu, Y. J.: Dissolved carbon export and CO_2 outgassing from the lower Mississippi River - Implications of future river carbon fluxes, Journal of Hydrology, 578, 10.1016/j.jhydrol.2019.124093, 2019.

Renaud, F. G., Syvitski, J. P. M., Sebesvari, Z., Werners, S. E., Kremer, H., Kuenzer, C., Ramesh, R., Jeuken, A., and Friedrich, J.: Tipping from the Holocene to the Anthropocene: How threatened are major world deltas?, Current Opinion in Environmental Sustainability, 5, 644-654, 10.1016/j.cosust.2013.11.007, 2013.

Richardson, J. L., Desai, A. R., Thom, J., Lindgren, K., Laudon, H., Peichl, M., Nilsson, M., Campeau, A., Järveoja, J., Hawman, P., Mishra, D. R., Smith, D., D'Acunha, B., Knox, S. H., Ng, D., Johnson, M. S., Blackstock, J., Malone, S. L., Oberbauer, S. F., Detto, M., Wickland, K. P., Forbrich, I., Weston, N., Hung, J. K. Y., Edgar, C., Euskirchen, E. S., Bret-Harte, S., Dobkowski, J., Kling, G., Kane, E. S., Badiou, P., Bogard, M., Bohrer, G., O'Halloran, T., Ritson, J., Arias-Ortiz, A., Baldocchi, D., Oikawa, P., Shahan, J., and Matsumura, M.: On the Relationship Between Aquatic CO2 Concentration and Ecosystem Fluxes in Some of the World's Key Wetland Types, Wetlands, 44, 10.1007/s13157-023-01751-x, 2024.

River, I. I. C. f. t. P. o. t. D.: On the implementation of the joint program of measures in the Danube River basin 2018, 2018.

Rocher-Ros, G., Gomez-Gener, L., Jativa, C., Lannergård, E. E., Laudon, H., Lupon, A., Martí, E., Peñarroya, X., Sponseller, R. A., and Bernal, S.: Emerging patterns of CO_2 : O_2 dynamics in rivers and their link to ecosystem carbon processing, Limnology and Oceanography Letters, 10.1002/lol2.70057, 2025.

Rode, M., Wade, A. J., Cohen, M. J., Hensley, R. T., Bowes, M. J., Kirchner, J. W., Arhonditsis, G. B., Jordan, P., Kronvang, B., Halliday, S. J., Skeffington, R. A., Rozemeijer, J. C., Aubert, A. H., Rinke, K., and Jomaa, S.: Sensors in the Stream: The High-Frequency Wave of the Present, Environmental Science and Technology, 50, 10297-10307, 10.1021/acs.est.6b02155, 2016.

Romanova, Y., Shakirzanova, Z., Ovcharuk, V., Todorova, O., Medvedieva, I., and Ivanchenko, A.: Temporal variation of water discharges in the lower course of the Danube River across the area from Reni to Izmail under the influence of natural and anthropogenic factors, Energetika, 65, 144-160, 10.6001/energetika.v65i2-3.4108, 2019.

Rosentreter, J. A., Laruelle, G. G., Bange, H. W., Bianchi, T. S., Busecke, J. J. M., Cai, W.-J., Eyre, B. D., Forbrich, I., Kwon, E. Y., Maavara, T., Moosdorf, N., Najjar, R. G., Sarma, V. V. S. S., Van Dam, B., and Regnier, P.: Coastal vegetation and estuaries are collectively a greenhouse gas sink, Nature Climate Change, 13, 579-587, 10.1038/s41558-023-01682-9, 2023.

Sabater, S., Timoner, X., Borrego, C., and Acuña, V.: Stream Biofilm Responses to Flow Intermittency: From Cells to Ecosystems, Frontiers in Environmental Science, 4, 10.3389/fenvs.2016.00014, 2016.

Shangguan, Q. P., Degrandpre, M. D., Hall, R. O., Jr., and Payn, R. A.: Freshwater carbonate buffering revisited, Limnology and Oceanography Letters, 10, 619-635, 10.1002/lol2.70047, 2025.

Solano, V., Duvert, C., Birkel, C., Maher, D. T., Garcia, E. A., and Hutley, L. B.: Stream respiration exceeds CO_2 evasion in a low-energy, oligotrophic tropical stream, Limnology and Oceanography, 68, 1132-1146, 10.1002/lno.12334, 2023.

Tiegs, S. D., Costello, D. M., Isken, M. W., Woodward, G., McIntyre, P. B., Gessner, M. O., Chauvet, E., Griffiths, N. A., Flecker, A. S., Acuña, V., Albariño, R., Allen, D. C., Alonso, C., Andino, P., Arango, C., Aroviita, J., Barbosa, M. V. M., Barmuta, L. A., Baxter, C. V., Bell, T. D. C., Bellinger, B., Boyero, L., Brown, L. E., Bruder, A., Bruesewitz, D. A., Burdon, F. J., Callisto, M., Canhoto, C., Capps, K. A., Castillo, M. M., Clapcott, J., Colas, F., Colón-Gaud, C., Cornut, J., Crespo-Pérez, V., Cross, W. F., Culp, J. M., Danger, M., Dangles, O., de Eyto, E., Derry, A. M., Villanueva, V. D., Douglas, M. M., Elosegi, A., Encalada, A. C., Entrekin, S., Espinosa, R., Ethaiya, D., Ferreira, V., Ferriol, C., Flanagan, K. M., Fleituch, T., Shah, J. J. F., Frainer, A., Friberg, N., Frost, P. C.,

Garcia, E. A., Lago, L. G., Soto, P. E. G., Ghate, S., Giling, D. P., Gilmer, A., Gonçalves, J. F., Jr., Gonzales, R. K., Graça, M. A. S., Grace, M., Grossart, H. P., Guérold, F., Gulis, V., Hepp, L. U., Higgins, S., Hishi, T., Huddart, J., Hudson, J., Imberger, S., Iñiguez-Armijos, C., Iwata, T., Janetski, D. J., Jennings, E., Kirkwood, A. E., Koning, A. A., Kosten, S., Kuehn, K. A., Laudon, H., Leavitt, P. R., da Silva, A. L. L., Leroux, S. J., Leroy, C. J., Lisi, P. J., MacKenzie, R., Marcarelli, A. M., Masese, F. O., McKie, B. G., Medeiros, A. O., Meissner, K., Milisa, M., Mishra, S., Miyake, Y., Moerke, A., Mombrikotb, S., Mooney, R., Moulton, T., Muotka, T., Negishi, J. N., Neres-Lima, V., Nieminen, M. L., Nimptsch, J., Ondruch, J., Paavola, R., Pardo, I., Patrick, C. J., Peeters, E., Pozo, J., Pringle, C., Prussian, A., Quenta, E., Quesada, A., Reid, B., Richardson, J. S., Rigosi, A., Rincón, J., Rîsnoveanu, G., Robinson, C. T., Rodríguez-Gallego, L., Royer, T. V., Rusak, J. A., Santamans, A. C., Selmeczy, G. B., Simiyu, G., Skuja, A., Smykla, J., Sridhar, K. R., Sponseller, R., Stoler, A., Swan, C. M., Szlag, D., Teixeira-de Mello, F., Tonkin, J. D., Uusheimo, S., Veach, A. M., Vilbaste, S., Vought, L. B. M., Wang, C. P., Webster, J. R., Wilson, P. B., Woelfl, S., Xenopoulos, M. A., Yates, A. G., Yoshimura, C., Yule, C. M., Zhang, Y. X., and Zwart, J. A.: Global patterns and drivers of ecosystem functioning in rivers and riparian zones, Science Advances, 5, 10.1126/sciadv.aav0486, 2019.

Tschikof, M., Gericke, A., Venohr, M., Weigelhofer, G., Bondar-Kunze, E., Kaden, U. S., and Hein, T.: The potential of large floodplains to remove nitrate in river basins - The Danube case, Science of the Total Environment, 843, 10.1016/j.scitotenv.2022.156879, 2022.

Vachon, D., Sadro, S., Bogard, M. J., Lapierre, J. F., Baulch, H. M., Rusak, J. A., Denfeld, B. A., Laas, A., Klaus, M., Karlsson, J., Weyhenmeyer, G. A., and Giorgio, P. A.: Paired O_2 – CO_2 measurements provide emergent insights into aquatic ecosystem function, Limnology and Oceanography Letters, 5, 287-294, 10.1002/lol2.10135, 2020.

van der Knaap, J., Harpenslager, S. F., Aben, R. C. H., Weideveld, S. T. J., van Giersbergen, Q., van Dijk, G., Wintjen, P., Buzacott, A. J. V., Fritz, C., Kruijt, B., and Kosten, S.: Disproportionately High Contribution of Ditches to Landscape Greenhouse Gas Emissions in Drained Peatlands, Ecosystems, 28, 10.1007/s10021-025-01005-3, 2025.

van Heuven, S., Pierrot, D., Rae, J. W. B., Lewis, E., and Wallace, D. W. R.: MATLAB Program Developed for CO_2 System Calculations, Carbon Dioxide Information Analysis Center, Oak Ridge National Laboratory, U.S. Department of Energy, Oak Ridge, Tennessee, 10.3334/CDIAC/otg.CO2SYS_MATLAB_v1.1, 2011.

Vorobyev, S. N., Kolesnichenko, L. G., Kolesnichenko, Y., Prokushkin, A. S., Lugovaya-Dolmatova, A., Karlsson, J., and Pokrovsky, O. S.: Floodplain carbon dioxide emissions strongly exceed those of the main river stem: A case study of the Ob River, western Siberia, Journal of Hydrology, 638, 10.1016/j.jhydrol.2024.131468, 2024.

Weiss, R. F.: Carbon dioxide in water and seawater: the solubility of a non-ideal gas, Marine Chemistry, 2, 203-215, 10.1016/0304-4203(74)90015-2, 1974.

Xue, H., Ding, H., Han, X. K., Lang, Y. C., Wang, T. J., Li, P., Qiao, M. R., Liu, D. D., Liu, Z. H., and Liu, C. Q.: Ditches as key players in carbon emissions in managed *Phragmites*-dominated wetland, Journal of Hydrology, 647, 10.1016/j.jhydrol.2024.132355, 2025.

Zuijdgeest, A., Baumgartner, S., and Wehrli, B.: Hysteresis effects in organic matter turnover in a tropical floodplain during a flood cycle, Biogeochemistry, 131, 49-63, 10.1007/s10533-016-0263-z, 2016.

Zurbrügg, R., Wamulume, J., Kamanga, R., Wehrli, B., and Senn, D. B.: River-floodplain exchange and its effects on the fluvial oxygen regime in a large tropical river system (Kafue Flats, Zambia), Journal of Geophysical Research: Biogeosciences, 117, 10.1029/2011jg001853, 2012.